Progress in Polymer Science 91 (2019) 141–168

Contents lists available at ScienceDirect

Progress in Polymer Science

journal homepage: www.elsevier.com/locate/ppolysci

Polymeric composites for powder-based additive manufacturing: Materials and applications

Shangqin Yuan, Fei Shen, Chee Kai Chua*, Kun Zhou*

Singapore Centre for 3D Printing, School of Mechanical and Aerospace Engineering, Nanyang Technological University, 50 Nanyang Avenue, Singapore 639798, Singapore

ARTICLE INFO

Article history:
Available online 7 November 2018

Keywords:
Additive manufacturing
3D printing
Selective laser sintering
Powder-based
Polymeric composites

ABSTRACT

As one of the most important categories in the additive manufacturing (AM) field, powder-based techniques, such as selective laser sintering, electron beam melting and selective laser melting, utilize laser or electronic beams to selectively fuse polymeric, metallic, ceramic or composite powders layer-by-layer into desired products according to their computer-aided design models. With unique mechanical, thermal, electrical, biocompatible and fire-retardant properties, polymeric composite materials for powder-based AM have been attracting intensive research interests because of their potential for a wide variety of functional applications in aerospace, automobile, marine and offshore, medical and many other industries.

This article provides a comprehensive review of the recent progress on polymeric composite materials, their powder preparation for AM, and functionalities and applications of their printed products. It begins with the introduction of thermoplastic polymers that have been used as the main matrices of the polymeric composites and various composite reinforcements such as metallic, ceramic, carbon-based fillers and polymer blends for strengthening and functionality purposes. Discussion is then made on the processes for manufacturing such polymeric composites into powder form, which include shear pulverization, solution-based methods and melt compounding methods, with a focus on their advantages, limitations and challenges in terms of their productivity and processibility as well as powder printability. Thereafter, the properties and functionalities of the printed products and their various intriguing applications particularly in biomedical (anatomical models, tissue engineering and drug delivery), aerospace, automobile, military, energy and environmental, acoustic devices and sports equipment are highlighted. Finally, this review is concluded with an outlook on polymeric composites for powder-based AM, new opportunities, major challenges and possible solutions.

Contents

* Corresponding authors.
E-mail addresses: mckchua@ntu.edu.sg (C.K. Chua), kzhou@ntu.edu.sg (K. Zhou).

https://doi.org/10.1016/j.progpolymsci.2018.11.001
0079-6700/

1. Introduction

Additive manufacturing (AM) or three-dimensional (3D) printing techniques are emerging to initiate a new round of manufacturing revolution by providing greater freedom for design and fabrication of customized products with complex geometries [1–5]. The 3D model of an object is constructed through computer-aided design (CAD) and mathematically sliced into many thin layers, according to the automatic deposition and scanning process for its various cross sections [6–10]. Over the years, AM has branched out from primarily serving as a prototyping technique, to the production of functional parts and end-use products [11–14].

Indeed, polymers and their composites for AM have been a rising and booming field, as demonstrated from an increasing number of related research works published (Fig. 1). According to the status of raw materials used, AM techniques could be classified into three categories: liquid-based, solid-based and powder-based ones. Powder-based AM techniques offer several advantages over other techniques such as fused deposition modeling (FDM), stereolithography, polyjet and hybrid-printing processes by easing the access of new types of polymers or polymeric composites for functional applications without requiring support structures as the printed parts are supported by their surrounding unfused powders [15–17].

Selective laser sintering (SLS), binder jetting and multi-jet fusion are the typical powder-based systems for polymeric materials, where a thin layer of powders is deposited on the build platform, followed by tracing of the cross-sectional area of each layer using a heat source or plastic binders to fuse or bind it with the previous layer [18]. SLS employs a CO_2 laser as the heat source to selectively melt the powders and fuse them under a pressure-free condition [19,20]. Binder jetting uses a printhead to selectively dispense liquid binders to glue powders in a pre-deposited powder layer on the building platform. Multi-jet fusion, a process recently developed by the Hewlett-Packard company, continues the system of recoating powders and selectively dispensing fusion agents, which can effectively absorb heat to accelerate the melting and fusion of powders. This process possesses the advantages of high productivity and low specific cost (cost per unit volume) in terms of energy and material consumptions [13,17,21]. In contrast, other techniques usually require additional support structures for overhanging features and thin walls, resulting in that an additional post-processing is necessary for removal of the support structures, and thus their productivity and specific cost are affected by the forming mechanism and feeding materials.

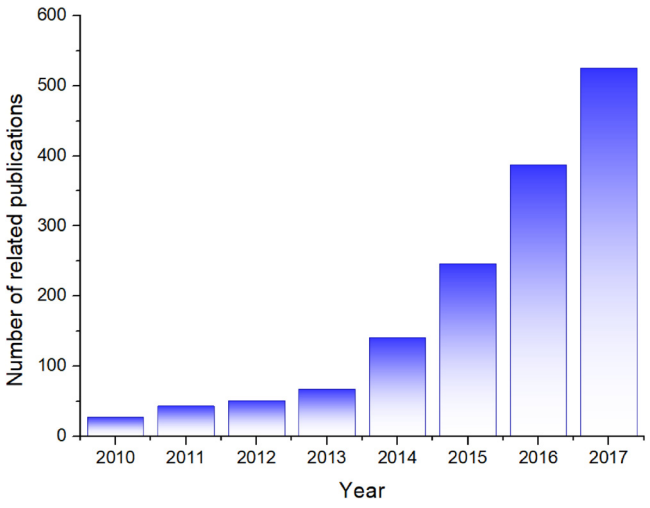

Fig. 1. Statistical data of the articles about the topics of polymers or their composites for AM techniques published during 2010-2018. The data was compiled from the ISI database on 20 August 2018.

Polymers and polymeric composites in AM have emerged as promising materials for a broad spectrum of research works and commercial applications owing to their unique physico-chemical properties and characteristics such as light-weight, cost-effectiveness, ease of process and variability of compositions. A wide range of reinforcements, which can be classified into four groups: metallic, ceramic, carbon-based fillers and organic additives, have been explored for development of polymeric composites. Reinforcements in a polymeric composite can enable the tailoring of its characteristics, such as surface chemistry [22], crystallinity [23–25], mechanical strength [25–27], specific heat absorption [25], heat dispersion or fire-retardancy, and electrical and thermal conductivities [28]. Thus, it is urgently desirable to apply functional composite materials in powder-based AM for novel functionalities of printed parts [22,29–33].

The research in composite powders has focused on the powder preparation processes such as cryogenic ball milling, wet grinding-rounding, emulsion-precipitation, dissolution-precipitation and spray drying. The preparation process of composite powders often determines their morphology, size distribution and constituents as well as the distribution of fillers within the polymeric matrix. These factors significantly influence the powder behaviors during printing, such as the flowability, surficial, thermal and rheological properties, as well as the performances of printed parts [34]. Thanks to the addition of reinforcements and the corresponding process optimization and post-process, the applications of printed parts have been extended to various fields due to the improved multi-functionalities in the aspects of mechanical, thermal, electrical properties, biocompatibility, etc.

This article provides a comprehensive review on the current status, challenges and emerging applications of polymeric composites for the powder-based AM techniques, particularly the powder fusion processes. It starts with a broad overview of various candidate materials and the strategies of their powder preparation capable of massive production, followed by discussion on the properties of printed composite products over a wide spectrum of functionalities encompassing mechanical, electrical, thermal, fire-retardant properties, bio-related performances, etc. The intriguing applications of the printed products are then highlighted, particularly in the four major themes: aerospace and military industries, biomedical and healthcare engineering, water treatment and energy storage, sports equipment and acoustic devices. Finally, the perspectives are presented on the currently faced challenges in the development of composite powders, the limitations of fabrication techniques and the future research directions.

2. Materials

A wide range of powders including ceramics and polymers can be processed by the powder-based binding process via binder jetting; however, binder selection is a key factor in successful part fabrication. Three different types of binders are commonly used in the binder jetting method: water-based binders (e.g., commercial ZB54, Z Corporation) [35], phosphoric and citric acid-based binders [36], and polymer solution binders [37]. To adjust the fluidic properties of these organic suspension binders so as to be compatible with the type of a jetting head (e.g., thermal or piezoelectric head), the viscosity and surface tension must be in the ranges from 5 to 20 Pa.s and from 35 to 40 mJ/N, respectively. To obtain the suitable ranges, the Ohnesorge number is used, which is defined as the ratio of $\sqrt{W_e}/R_e$ where W_e is the Weber number given by $v^2 r\rho/\sigma$ with r being the characteristic length, v the fluid velocity, σ the surface tension and ρ the fluid density and R_e is the Reynolds number given by $vr\rho/\eta$ with η being the dynamic viscosity of the fluid; i.e., $\sqrt{W_e}/R_e = \eta/\sqrt{\sigma\rho r}$ [38]. The Ohnesorge number should be between 0.1 and 1 [39]. The types of powders need to possess sufficient flowability and wettability to ensure a uniform deposition and confirm effective wetting during inkjet printing process. Therefore, the binder formulations and powder characteristics determine the process parameters such as the velocity and path of the jetting heads, the initial size of the droplets as well as chemical affinity between powders and binders.

Binder jetting is a universal and well-established approach to fabricate 3D parts using different combinations of powders and binders [40]. Although polymeric binders have been widely used to manufacture composite parts such as ceramic/polymer, glass/polymer and carbon fiber/polymer parts, they often have a low resolution and poor mechanical strength. Thus, as compared with binder jetting, the powder-bed fusion processes have proven to possess a greater potential for manufacturing functional parts for end-use applications.

Thermoplastics are predominately applied in the powder-bed fusion processes such as SLS and multi-jet fusion, as these polymers are capable of being reshaped and processed upon a heating-cooling cycle [26,41–47]. However, the powder-bed fusion processes have stringent requirements for polymeric materials (in both bulk and powder forms) that affect process operating parameters and effectiveness. As illustrated in Fig. 2, the recyclability of the used polymeric powders is related to their molecular properties (e.g., molecular weight, weight distribution, functional groups, molecular bonds and chemical oxidation); the sintering window and sintering stable range of the polymeric materials in printing are determined by their thermal properties (e.g., heat capacity, latent heat, transition temperatures, expansion coefficient, thermal decomposition and thermal conductivity), rheological properties (e.g., storage and loss moduli, surface tension and melt viscosity), and optical properties (transmission, absorption, and reflection); the deposition rate and layer thickness of the polymeric powders are determined by the flow properties (e.g., packing factor and avalanche angle). A good understanding of such properties is important to developing a new type of printable powders and determining their optimal printing process parameters [29,48–51].

Polymers for powder-bed fusion systems are mainly semi-crystalline thermoplastics, but may also be amorphous thermoplastics, dual-segment thermoplastics or elastomers [13]. A semi-crystalline polymer contains both amorphous and crystalline phases, and thus the critical glass, melting and recrystallization transitions could be easily identified [52–54]. As pre-heating could promote a polymer from the glassy to viscous state, the laser could easily trigger the polymer into its molten state, allowing it to remain at that temperature for sufficient time to minimize thermal stress-induced negative effects after consolidation. The bed temperature of a semi-crystalline polymer is often set just below the onset of the melting peak T_m and above the onset of the recrystallization peak T_r and this temperature range is defined as the sintering window of a polymer (Fig. 3a) [55,56]. In comparison, an amorphous polymer has no significant phase transfer upon a heating-cooling process and thus usually lacks critical melting and recrystallization transitions to identify the sintering window and bed temperature. For the near fully crystalline polymers, large thermal gradients during the phase transition often induce the dramatic curling and unexpected volume shrinkage of the printed products.

The flow and optical properties of the powders are also significant to determine process parameters such as layer thickness and deposition rate upon powder dispersion. The flowability of powders is attributed to their size distribution and morphology, which can be identified by the circularity versus roundness (Fig. 3b) [53,57], and can be directly evaluated by the avalanche angle and packing factor [58,59].

The energy absorbed from the laser is used to melt and fuse powders as well as retain the process temperature within the

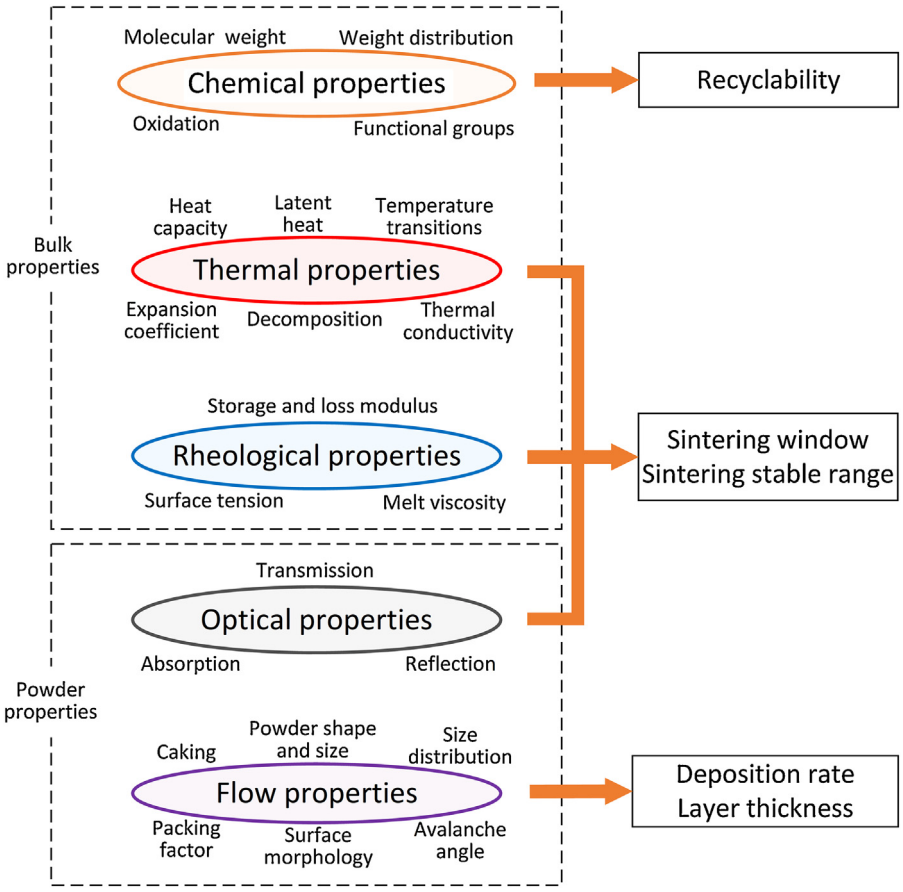

Fig. 2. Relationship between the properties of materials in bulk and powder forms and the process operating parameters and effectiveness.

stable sintering region [60]. A stable sintering region (SSR) was introduced to describe the optimum temperature range for a successful sintering process. SSR is usually defined as the range from melting temperature to onset of decomposition temperature for a specific polymer [61]. The energy density of the laser captures the net-effects of its power, beam size, scanning speed, hatching space and the powder layer thickness, as given by the form $E = P/f(v, D, H, \lambda)$, where P is the laser power, v is the laser scanning speed, D is the laser beam diameter, H is the laser hatching space and λ is the powder layer thickness [56,60]. The energy absorption capability of powders is associated with their light absorption and scattering effects [62]. Overheating, insufficient heating and poor material fusion usually cause problems such as thermal stress-induced warping, poor interlayer bonding, and balling effect, respectively (Fig. 3c) [63,64].

The properties of macromolecules such as molecular configuration, molecular weight, polydispersity and intermolecular bonding influence their melt behaviours, mechanical behaviours, aging stability and recyclability over the heating-cooling cycle. For instance, a polymer with low molecular weight and weak intermolecular bonding usually has relatively low crystallinity and melt viscosity, resulting in the ease of consolidation. Nevertheless, a polymer with high molecular weight was suggested to improve mechanical properties, particularly elongation at break [66].

The thermal oxidation-induced degradation, chain growth and permanent recrystallization are the main mechanisms of polymer aging, which limits the recyclability and mechanical performance of printed parts. The consolidation of the aged polymeric powders cannot be optimized, resulting in inferior surface qualities and poor mechanical properties of printed parts. Moreover, some of semi-crystalline polymers experience permanent recrystallization upon cooling, which also causes powder aging and increases the energy barrier of melting for the recycled powders. Recently, the approaches to improving the thermal stability and preventing powder aging include the addition of oligomers or short polymers chains with free amine and carboxylic groups, the utilization of stabilizing agents such as phosphates, hindered phenols and thioethers, and the combination with antioxidants such as hydroquinones, sulfur components and hindered amines.

In a summary, polymeric materials favorable for the powder-bed fusion process should meet various requirements including proper molecular weight, semi-crystalline structure, a sharp melting peak, a narrow melting range, medium melt viscosity, a wide glass temperature window, desired recrystallization behaviour, high thermal stability and good recyclability [47,67,68].

2.1. Polymeric matrices

As shown in Fig. 4, the main categories of engineering polymers for the powder-based AM include semi-crystalline thermoplastics (e.g., polyamides (PAs), polypropylene (PP), Polyaryletherketone (PAEK), polyethylene (PE), and polybutylene terephthalate (PBT)), amorphous thermoplastics (e.g., polycarbonate (PC) and polystyrene (PS)), and thermoplastic elastomers (TPEs) (e.g., ester-based polyurethane (PU)). Additionally, biocompatible thermoplastics are attractive polymers for unique applications in tissue engineering (e.g., polyvinyl alcohol (PVA), poly- ε -caprolactone (PCL), poly(hydroxybutyrate-co-hydroxyvalerate) (PHBV), polylactide (PLA), polyglycolide (PGA), and their co-polymers [69,70].

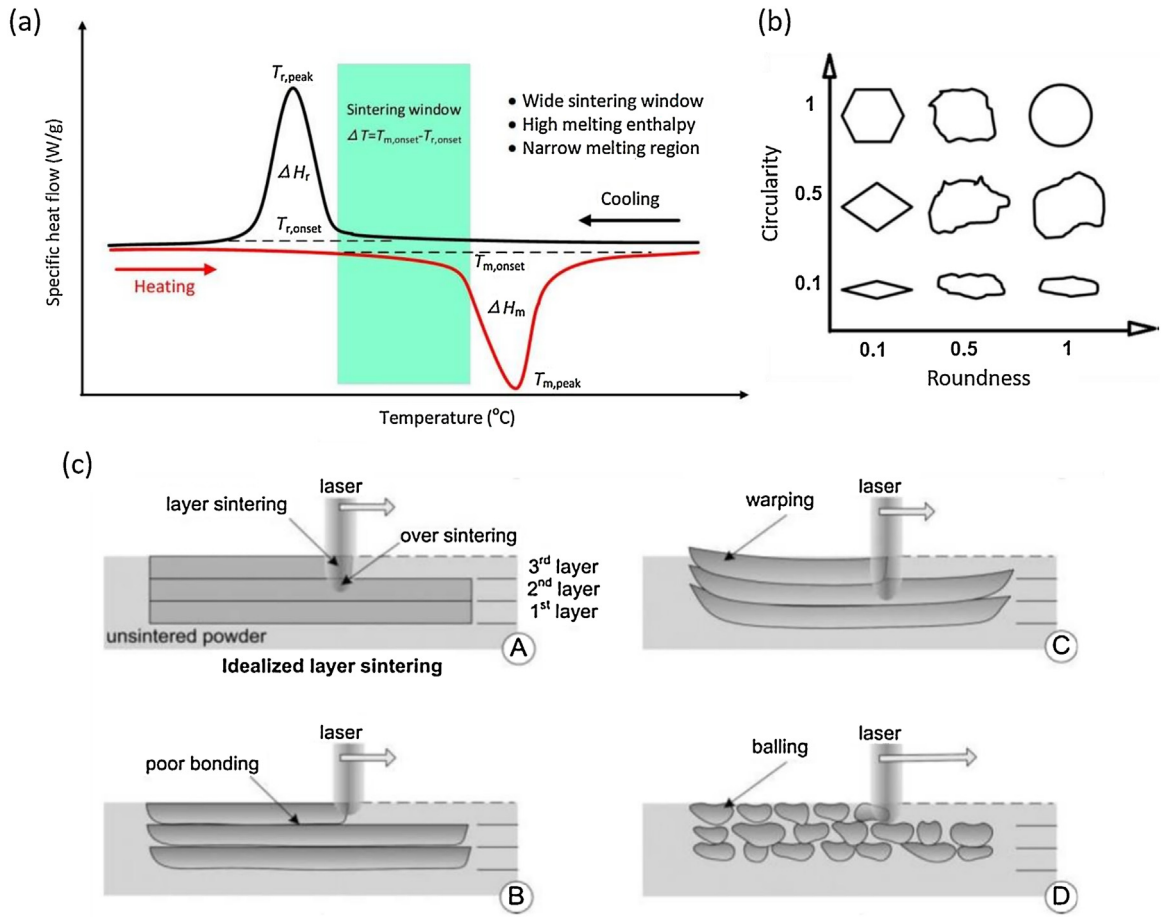

Fig. 3. (a) Typical differential scanning calorimetry (DSC) diagram of a semi-crystalline polymer with the sintering window, melting peak and recrystallization peak; (b) circularity versus roundness; (c) effects induced by the laser energy density (A: normal; B: insufficient heating; C: overheating; D: poor material fusion) [65]. Copyright 2009. Adapted with permission from John Wiley & Sons, Inc.

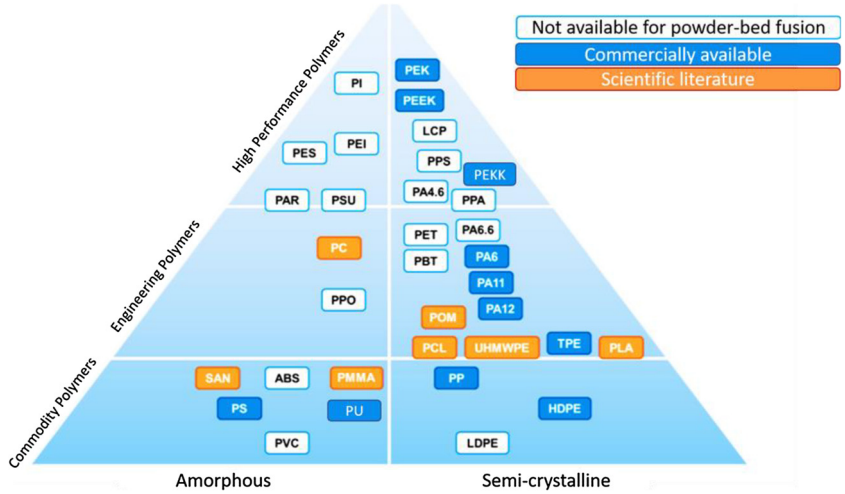

Fig. 4. The representative thermoplastics for the SLS or multi-jet fusion process.

2.1.1. Semi-crystalline polymers

PAs or PA-based thermoplastic composites occupy 95% of the commercial market of powder-based fusion processes including SLS and multi-jet because PA12 and PA11 are typical semi-crystalline thermoplastics that satisfy the critical requirements for these processes [13,71,72]. Most of PAs have a moderate glass transition T_g of 40 °C, and PA11 and PA12 exhibit sharp melting ranges of 183–190 °C and 176–188 °C, respectively [73,74]. A large sintering window of PA12 allows it to slowly cool down, resulting in the delaying and minimization of its re-crystallization to prevent the accumulation of residual stresses that can cause the distortion of parts [75]. In contrast, PA11 with a narrow sintering window exhibits a relatively high tendency to distort and warp due to the large thermal stresses induced upon solidification

to recrystallization [76]. PA11 experiences rapid re-crystallization and degradation during pre-heating due to the formation of hydrogen bonds among molecular chains, resulting in highly ordered crystalline phase [77]. Although the ultimate tensile strength of laser-sintered PA11 (about 50 MPa) is greater than that of PA12 (45 MPa), PA12 is easy to process and recycle and thus widely used for prototyping [78]. PA6 is also attractive for commercialization in the SLS system due to its great plastic deformation and controllable elastic recovery under an elevated temperature [79]. However, as compared with PA12 and PA11, PA6 exhibits a relatively high melting point at 223 °C and increased melt viscosity, which creates a process barrier due to sintering kinetics [77,80].

PAs are susceptible to the thermal history-induced residual stresses and micro-structural crystalline change [81]. Over several thermal cycles, the condensation of active amine and carboxylic groups occurs in PAs and causes molecular chain growth, resulting in the increased melting point and melts viscosity as well as the degradations of powder properties.

PAEKs are a family of high-performance polymers with superior properties such as outstanding mechanical performances, excellent thermal and chemical resistance, low moisture absorption, and good resistance to creep and fatigue [82]. As candidate materials for SLS, PAEKs include PEEK, PEKK and PEK based on their chemical conformations [83,84].

PEK and PEEK are semi-crystalline thermoplastics with a good strength up to 90 MPa, Young's modulus of about 5 GPa and excellent thermal and chemical resistance [87–90]. Berrretta et al. [82,85–88] systematically investigated the processability of PEK and PEEK through the aspects of their thermal transitions, powder flowability, melt viscosity, particle coalescence and mechanical performances of laser-sintered parts. PEK (EOS HP3) shows the critical points of T_m, T_r and T_g at 372 °C, 334 °C and 164 °C, respectively, and therefore its pre-heating temperature falls within a narrow range of 343–357 °C [89]. PEEK exhibits the lower critical points of T_m and T_g at 343 °C and 143 °C, respectively but a broad range of T_g from 310 °C to 170 °C. These temperature transitions T_m and T_g indicate that PEEK provides a wider sintering window and a lower pre-heating temperature than PEK. The build chamber for holding sintered PEEK and PEK parts need to be retained at an operation temperature of 250–260 °C in order to minimize thermal stresses-induced warping and distortion. Thus, the machine system must meet stringent requirements in the aspects of hardware protection as well as the pre-heating and cooling stability.

PEKK exhibits excellent biocompatibility and chemical resistance, with the density and stiffness similar to those of bone [90,91]. The T_g and T_m of PEKK are 162 °C and 340 °C, respectively, and the desired isothermal temperature of crystallization falls within the range of 305–315 °C [92]. However, the recrystallization of PEKK is greatly accelerated to complete in a short period and thus significantly induce localized thermal stresses as compared with that of PEEK [92]. The laser-sintered parts from the PAEK family exhibit the Young's modulus of 3.2 GPa, the tensile strength of 70 MPa and the service temperature up to 260 °C and possess large potential to be used in aerospace and automotive components [91], bio-medical implants [93] and zero-loading parts for tissue engineering owing to their good biocompatibility and bioactivity [94].

The polymers in the PAEK family undergo significantly degradation and possess poor recyclability due to thermo-oxidation and the deleterious effects of chain scission after the heating-cooling cycle [13,95]. The used PEK powders exhibit the increased T_g and T_r, which require a further increase of the pre-heating and chamber temperature that can induce huge barriers for the sintering process.

PP exhibits great chemical resistance to dilute or concentrated acids, alcohols, bases and mineral oils, and thus its printed components are appropriate candidates for corrosion resistant applications [50,68,96]. In addition, PP is biocompatible, and its components could be used as permanent surgical implants [97]. Fiedler et al. [98] and Wegner et al. [99] evaluated the bulk and powder properties of various PP homopolymers and copolymers, and then proposed the powder development and surface modification approaches to prepare laser-sinterable PP powders.

PE is another category of thermoplastic polymers; its micron powders are widely used for spray coating to improve the surface hydrophobicity of products. Recently, PE has also been emerging to be applicable for the SLS system. In particular, high-molecular-weight PE (HMWPE) exhibits biocompatible and bendable mechanical behaviours. The blended powders consisting of PE and PA (PrimePart ST from EOS) are applied in a laser sintering system to produce rubber-like components with improved mechanical strength and flexibility as compared with neat PE.

PCL is a biodegradable polyester with the potential to be applied for bone and cartilage repair [98,100]. The ring-open polymerization of ε-caprolactone in PCL yields a semi-crystalline polymer with a melting range of 58–63 °C and a glass transition temperature of 60 °C [63,101]. The molecular structure of homopolymer PCL consists of five nonpolar methylene groups and a single relatively polar ester group, which is degradable when the hydrolytically unstable aliphatic-ester linkage is present [101]. The degradation product is a caproic acid that can be found naturally in animal oils, and generally PCL is considered as non-toxic and biocompatible. However, the degradation period of homopolymer PCL is more than two years, and thus the copolymers of ε-caprolactone and dl-lactide are synthesized to accelerate the degradation rate of the polymer scaffold [102]. It is possible to modify the mechanical properties and degradation rate of PCL-PLA copolymer by tailoring its composition and conformation [103]. The mechanical properties of PCL scaffolds are also alterable through controlling the geometry and porosity (e.g., the porosity ranging from 51.1% to 80.9%) and their compressive stress ranges from 10 MPa to 0.6 MPa [104].

Poly(alpha-hydroxy-acid)s (PLAGAs) derived from lactic acid and glycolic acid are bioresorbable polymers and used in the reconstruction of temporary bone replacement for tissue regeneration [112]. A full range of copolymers with lactic acid and glycolic acid has large potential to be utilized as laser sintering materials. It is generally accepted that intermediate copolymers are much more unstable than homopolymers such as PLA and PGA.

2.1.2. Amorphous polymers

PS has been used as feeding stock in indirect laser sintering for casting mold fabrication; in particular, syndiotactic PS gains considerable attention because it is a cost-effective engineering polymer which has a relatively high melting range of above 270 °C [72,105], low dielectric constant, low permeability to gases and good chemical resistance [27]. However, laser-sintered PS cannot serve as structural materials for loading sustaining components due to its poor mechanical ductility and severe thermal degradation [106].

PC possesses extraordinarily good dimensional stability and high impact strength, which can be maintained over a wide range of temperature [100,101]. Unfortunately, PC is a typically hard thermoplastic with poor mechanical ductility and elasticity [100], and thus its polymeric blends or composites with improved toughness and elastic properties are practical and feasible for industrial usages [74,102].

2.1.3. Elastomers

Thermoplastic elastomers (TPEs) close the gap between soft rubbers and hard plastics, as they combine rubber-like flexible behaviours and moderate mechanical strengths comparable to those of hard plastics after being re-melted and re-shaped. They provide a solution for the powder-bed fusion process to fabricate elastomeric functional parts for applications in sports equipment, shoe midsoles, orthopedic insoles, etc.

TPEs can be block copolymers that contain at least one semi-crystalline hard block (e.g., PA) that endows sufficient mechanical strength and thermal stability and one soft block (e.g., polyether) that provides elastomeric flexibility. The glass transition T_g and mechanical strength of copolymeric elastomers are dependent on ratio of the hard segments to soft segments. Tuning the average block lengths of hard segments can monitor T_g and melt viscosity and thus influence the processability of a copolymer in the powder-based fusion process. A type of commercialized TPE powders comprises semi-crystalline hard blocks with well-defined chain lengths and amorphous-dominated soft blocks. This block copolymer is grindable in an efficient manner and the resulted powders exhibit great process reliability because the pre-designed block configuration can minimize the cross-amdidation reactions that can convert the block copolymer to a statistic copolymer.

Alternatively, another type of block copolymer via dual-segment thermoplastic PUs (TPUs) with elastomeric behaviours has also been introduced to the powder-based fusion system [49]. TPUs are segmented block polymers with the soft segments consisting either of polyether or polyester chains and the hard segments induced by the addition of a short-chain diol to an isocyanate [103]. Verbelen et al. [53] investigated the processability of various types of ester-based TPUs for laser sintering, focusing on their melting and volume change and their powder flow and coalescence upon process cycle. Plummer et al. [31] reported that un-sintered TPU powders do not experience significant aging effects in a heated build chamber and can thus be reused again.

2.2. Reinforcements

A wide spectrum of polymers has been used for powder-based AM; however, the production and applications of polymeric parts face many challenges arising from inferior mechanical properties, poor thermal stability, and limited consistency and repeatability. Consequently, increasing efforts have been devoted to reinforcing polymeric parts using functional reinforcements.

Reinforcements in polymeric matrices can be classified into four categories: (i) metallic fillers (e.g., aluminum and carbon steel) [107]; (ii) ceramic/glass fillers (e.g., silica, glass beads, clays and oxides) [108]; (iii) carbon-based fillers (e.g., carbon black, carbon nanotubes (CNTs), graphite and graphene) [109]; (iv) organic additives (e.g., PC, PS) [26,27]. The usage of composite powders in the powder-based AM techniques has demonstrated several advantages. Firstly, the addition of the reinforcements can help printed parts achieve improved mechanical strength, fire-retardancy, thermal conductivity, electrical conductivity, biocompatibility, piezoelectric properties, etc. Secondly, the addition of nanoparticles such as silica and CNTs can improve the flowability and light absorption capability of polymeric powders and then facilitate their deposition and fusion processes. Thirdly, through indirect laser sintering, the composite powders of refractory metal/polymer such as molybdenum (Mo)/PS can be processed at a low temperature range and the resulted green parts can then be obtained by burning the polymer phase. Table 1 lists various polymeric composite powders and their preparation methods and highlights the enhanced functional performances of the parts printed from them.

3. Processes for composite powder development

Various processes have been developed to manufacture composite powders, as summarized in Fig. 5, and their procedures determine the powder size, size distribution, morphology, composition and configuration and thus the operating parameters of the powder-based AM techniques. The composite powder manufacturing can be classified into single-step and multiple-step methods. Single-step method can directly process precursor materials into polymeric composite powders via one chemical or mechanical method (as highlighted in the blue boxes in Fig. 5). Nevertheless, the multiple-step methods additionally require a pre-process to prepare bulk polymeric composites (as highlighted in the yellow boxes in Fig. 5) or a post-treatment process such as adding coating layers on powders or both.

The single-step methods mainly include: (i) solid-state pulverization (e.g., cryogenic milling and wet grinding), (ii) solution-based methods (e.g., emulsion-evaporation and dissolution-precipitation), (iii) spray drying and (iv) pressure-free mechanical mixing (a simple and most widely applied approach for powder mixing). The multiple-step methods include: (i) melt-emulsion with rotating shearing, (ii) melt-compounding with ball milling or spray drying, (iii) solution intercalation with ball milling or spray drying, and (iv) a single-step method with post-coating. As summarized in Table 1, these powder manufacturing processes have focused on incorporating functional reinforcements such as metallic, carbon-based, ceramic fillers and organic additives with polymers to develop various AM-printable polymeric composite powders.

3.1. Solid-state shear pulverization

Solid-state shear pulverization is a type of environmentally benign process that applies high shear and compressive forces to bulk materials, resulting in their fragmentation and fusion in the solid state [162]. It is generally employed to mechanochemical modification of polymers [171–173], exfoliation and dispersion of fillers in polymeric nanocomposites [174,175], and recycling of used plastics [176]. Cryogenic milling and wet grinding are two typical shear pulverization processes to prepare polymeric composite powders according to the operational conditions [177–179]. Such processes can enhance filler distribution and modify powders due to the fact that the applied mechanical shear forces can promote material fusion and overcome the hardness mismatch between polymers and fillers [59,153,178–180].

3.1.1. Cryogenic milling

Cryogenic milling mainly uses ceramic or metallic balls or blades to break bulk polymers and fillers such as carbon fibers, nanoclays and carbon blacks at a low temperature below −50 °C, and then mixes or fuses them into composite powders containing a uniform distribution of fillers [48,162,181] (Fig. 5a to Fig. 6a). Powders of varied sizes can then be screened via sieving to narrow down their distribution to a desirable range. This process was successfully employed to blend PA12/PEEK [89,160], carbon fiber/PAEK [155], PA12/HDPE [158], HA/PEEK [181], HA/PVA [141] and HA/PE [144]. These composite powders possessed improved processability and functionality, compared with neat polymer powders. The constituent phases of the composite powders are well distributed and highly compacted through high-energy collision of milling balls or blades. However, these powders typically exhibit irregular morphology and low packing density that may induce their inferior fusion upon a laser sintering process. Furthermore, it is difficult to mill the elastomeric materials with T_g below −50 °C due to the retention of their rubbery behaviour. Another challenge is to overcome the agglomeration of nanoparticles so as to achieve a uniform dispersion within a polymer matrix. The pre-treatment of bulk nanocomposites is required to prepare for the stage of cryogenic milling [134,135].

3.1.2. Wet grinding

Wet grinding is a top-down approach to produce micro-particles and even nanoparticles for a variety of materials [59,178,179].

Table 1
Polymeric composite powders, preparation processes and purposes.

Filler		Matrix	Powder preparation method	Ref.	Purpose
Metallic	Al	PA12	Physical powder mixing	[107]	• Improved thermal and electrical conductivities and mechanical strength by metallic microparticles
	Carbon steel	PA12	Dissolution-precipitation	[42]	• Metallic green part fabricated by an indirect laser sintering process
	Stainless steel	PA12, PS	Ball milling	[111]	
	Mo	PA12	Cryogenic ball milling	[41,112]	• Polymer as a removable binder
	Cu	PMMA	Physical powder mixing	[113]	
Ceramic	Al_2O_3	PA12	Dissolution-precipitation	[114]	• Enhanced mechanical strength by micro-/nano-Al_2O_3 particles • Improved thermal stability and fire-retardancy
		PEEK	Melt-compounding	[108,115]	
		PS	Dispersion polymerization coating	[106]	• Ceramic green parts fabricated by an indirect laser sintering process
		PS	Physical powder mixing	[116]	
		PVA	Spray drying coating	[117]	• Coated polymer layer as a removable binder
	AlCuFeB	PA12	Physical powder mixing	[118]	• Enhanced tensile and impact strengths by quasicrystal nanoclays
	ZrO_2	PP	Dissolution-precipitation	[119]	
		PA6	Spray drying	[120]	• Improved thermal stability and fire-retardancy by inorganic nanoparticles such as SiO_2 and SiC and nanoclays
	Y_2O_3	PP	Dissolution-precipitation	[119]	
	SiO_2	PA11, PA12	Melt-compounding and ball milling	[78]	
		PA12	Emulsion-evaporation	[121]	• Improved impact strength, creep resistance, toughness and tensile strength
			Dissolution-precipitation	[25]	
		PEEK	Melt-compounding and ball milling	[115]	• $BaTiO_3$ polymeric nanocomposites with piezoelectrical properties for sensing and energy harvesting
	$BaTiO_3$	PA12	Melt-compounding and grinding	[122]	
	SiC	PA12	Physical powder mixing	[123]	
		PMMA	Spray drying coating	[124]	
	PTWs	PA12	Dissolution-precipitation	[123]	
	Glass	PA11	Physical powder mixing	[125,126]	
	Montmorillonite	PA11	Melt-compounding and ball milling	[33,78]	
		PA12	Melt-compounding and ball milling	[18]	
		PA12	Dissolution-precipitation	[127]	
		PS	Melt-compounding and ball milling	[128]	
	Rectorite	PA12	Dissolution-precipitation	[129]	
	Fly ash	PEEK	Melt compounding and ball milling	[93,130]	
	TiO_2	PEEK	Physical powder mixing	[131]	• TiO_2/PEEK nanocomposites for tissue engineering and medical device fabrication
		PA12	Dissolution-precipitation	[132]	• TiO_2/PA12 nanocomposites with high resistance to UV to prevent polymer aging • Increased thermal stability and elastic modulus
		PET, PEN	Cryogenic ball milling	[133]	• TiO_2 polymeric nanocomposite with porous structure fabricated for solar cell and energy harvesting
	CHA	PLLA	Emulsion-evaporation	[134,135]	• Bio-ceramics CHA and HA blended with PLLA and PCL for bioactive and biodegradable tissue scaffolds • PEEK mixed with bio-ceramics for permanent implants with improved cell attachment and growth • PVA and PMMA as binder materials to glue ceramic particles with biopolymer powders.
		PHVB	Emulsion-evaporation	[136]	
	HA	PEEK	Physical powder mixing	[9,131]	
		PA12	Melting-compounding and ball milling	[137]	
		PLLA	Physical powder mixing	[138]	
		PCL	Cryogenic ball milling	[139]	
			Physical powder mixing	[140]	
		PVA	Physical powder mixing	[9,141]	
		PMMA	Physical powder mixing	[142]	
		HDPE	Dissolution-precipitation	[143]	
			Melting-compounding and ball milling	[137]	
			Cryogenic ball milling	[144]	
	β-TCP	PLA	Physical powder mixing	[145]	
		PCL	Cryogenic ball milling	[146,147]	
			Physical powder mixing	[147]	
		PLGA	Cryogenic ball milling	[148]	
	BCP	PHVB	Emulsion-evaporation	[136]	
Carbon-based	CNTs	PA11	Melt-compounding and ball milling	[33]	• Improved laser energy absorption and powder fusion acceleration by CNTs and graphene • Enhanced thermal and electrical conductivities by CNTs • Improved mechanical properties including specific strength, impact toughness and ductility by CNTs • Enhanced thermal stability and fire-retardancy by CNTs and carbon fibers • Light-weight composites with excellent electrical conductivity but sacrificing of mechanical toughness and tensile strength. • Enhanced laser energy absorption by carbon black and graphite
		PA12	Dissolution-precipitation	[71,150]	
			Melting-compounding and ball milling	[151]	
	Carbon fiber	PA12	Melting-compounding and ball milling	[33,108,152]	
		PA12	Polymer coating/inflation	[153]	
		PA11	Melting-compounding and ball milling	[33,78,154]	
		PEKK	Cryogenic ball milling	[155]	
	Graphene	PA11	Ball milling	[44]	
			Melting-compounding and ball milling	[31]	
	Graphite	PMMA	Solution-intercalation and ball milling	[22]	

Table 1 (*Continued*)

Filler		Matrix	Powder preparation method	Ref.	Purpose
		PC	Ball milling	[156]	
		PEEK	Physical powder mixing	[157]	
	Carbon black	PA12	Ball milling	[43]	
Organic additives	HDPE	PA12	Physical powder mixing	[158,159]	• Improved mechanical strength and thermal stress resistance by blending PA6, PEEK or PC with PA • Improved processability of the composite powders with constituent PS and HDPE as binder materials at low melting temperature • Improved wear resistance and toughness with PC or PTEF as a strong phase in the PEEK matrix • Improved mechanical properties of PC, PS and PA12 parts via infiltration of epoxy resin • Improved transparency of SMMA parts by infiltration of epoxy resin • Casting mold materials for indirect laser sintering • Controllable flammability by fire-retardant additives • Drug delivery by biopolymeric composites
	PA6	PA12	Physical powder mixing	[79]	
	PS	PA12	Physical powder mixing	[72]	
	PEEK	PA12	Cryogenic ball milling	[160,161]	
	PC	PA12	Cryogenic ball milling	[161]	
	PC	PEEK	Cryogenic ball milling	[48]	
	PTEF	PEEK	Melting-compounding and ball milling	[162]	
	Epoxy	PC	Post-infiltration	[26]	
	Epoxy	PS	Post-infiltration	[27,163]	
	Epoxy	SMMA	Post-infiltration	[164]	
	Epoxy	PA12	Post-infiltration	[165]	
	SAN	PS	Cryogenic ball milling	[166]	
	Wax	PS	Post-infiltration	[167]	
	Wax	PA11	Post-infiltration	[168]	
	Brominated hydrocarbon	PA12, PA11	Melting-compounding and ball milling	[169]	
	Progesterone	PCL	Cryogenic ball milling	[170]	

PEEK: polyether ether ketone; Al: Aluminum; Mo: Molybdenum; Cu: Copper; Al_2O_3: Alumina; Mo: Molybdenum; SiC: Silicon carbide; Y_2O_3: Yttria; ZrO_2: Zirconiar; CaPs: calcium phosphates; HA: Hydroxyapatite; CHA: Carbonated hydroxyapatite; Montmorillonite with ideal composition in $[(Al_{3.5\text{-}2.8}Mg_{0.5\text{-}0.2})(Si_8)O_{20}(OH)_4]Ex_{0.5\text{-}1.2;}$ PMMA: Poly (methyl methacrylate); HDPE: High-density polyethylene; PTFE: Polytetrafluoroethylene; Potassium titanium whiskers; PET: Polyethylene terephthalate; PLGA: Poly(lactic-co-glycolic acid); PEN: Polyethylene naphthalate; PEKK: Polyether ketone ketone; SAN: Styrene-acrylonitrile copolymer; BCP: By-product of the burning of pulverized coal; SMMA: Styrene methyl methacrylate co-polymer; AlCuFeB: $Al_{59}Cu_{25.5}Fe_{12.5}B_3$ quasicrystalline.

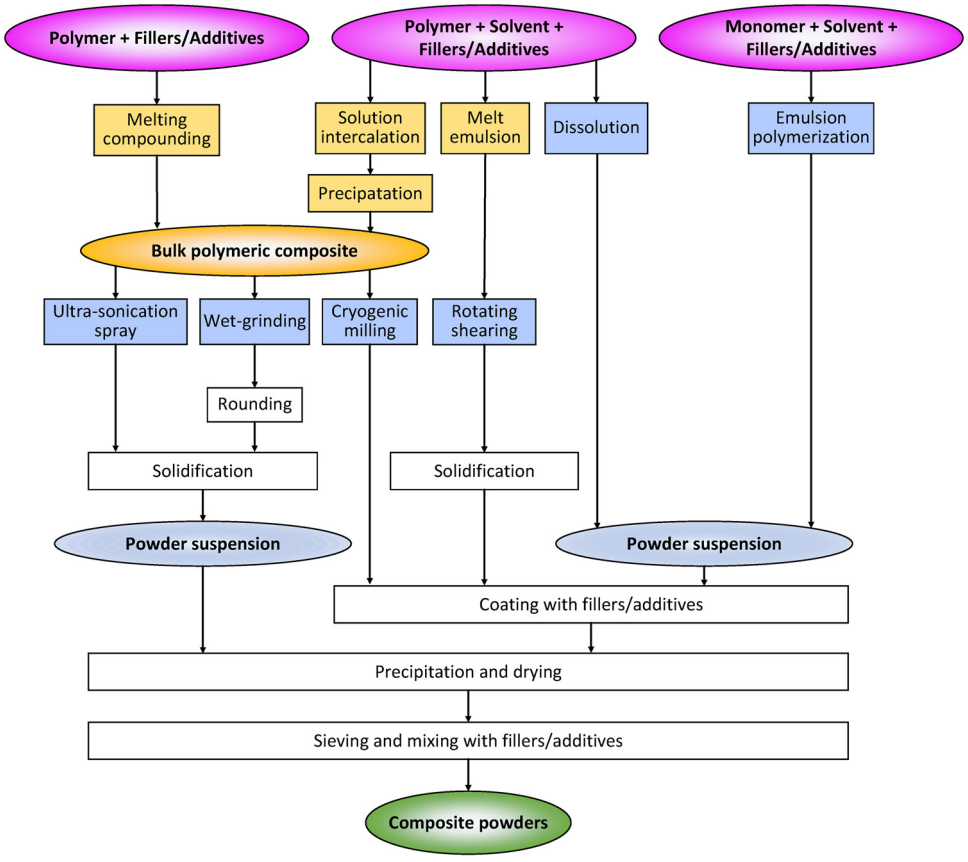

Fig. 5. Summary of various manufacturing processes for developing polymeric composite powders.

Besides the main step of wet grinding, this process also includes the other two steps: rounding of irregular microparticles and dry coating of flow agents (Fig. 6b). The low-viscous solvents and moderately reduced process temperature are monitored to control the ground particle size and size distribution. The modification of irregular powders in a downer reactor then allows for partial

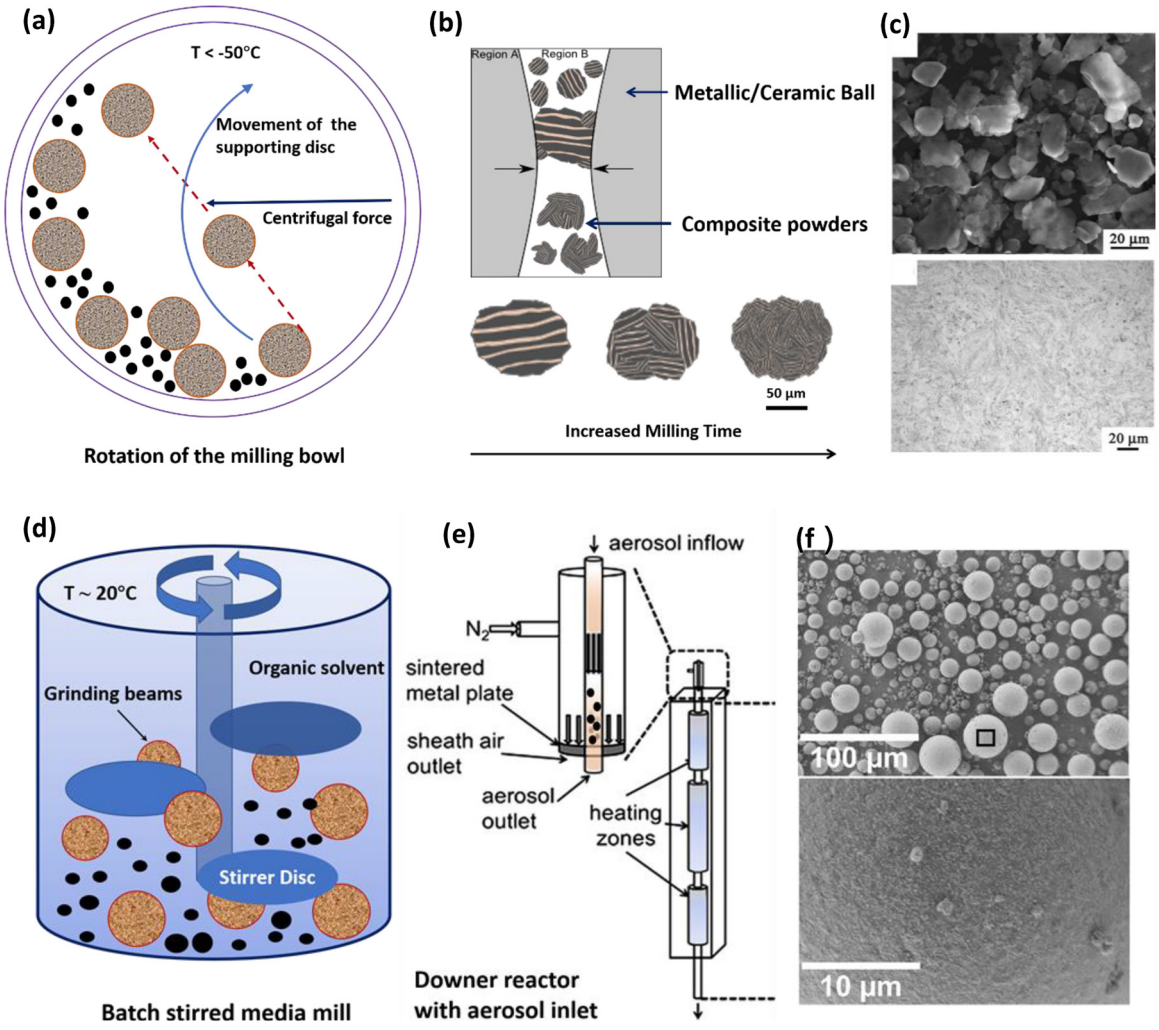

Fig. 6. (a) Illustration of a cryogenic ball milling process, (b) demonstration of microstructure changes of composites in the melt-compounding, and (c) the images of the powder morphology and microstructure [78]; (d) illustration of a wet-grinding process to produce composite powders, (e) downer reactor with aerosol inlet capable of rounding the grinded powders to spherical morphology, and (f) the images of powder morphologies [59]. Copyright 2012 Adapted with permission from Elsevier Inc. Copyright 2014 Adapted with permission from Elsevier Inc.

melting, rounding and subsequent solidification to obtain powders with spherical morphology. Afterwards, the dry coating of nanosilica or other flow agents is applied on the rounded powders using a tumbling mixer [59,179]. Using this process, Schmidt et al. [59,178] produced spherical composite powders of PS, PBT, POM (Polyoxymethylene) and PEEK coated with nanosilica. Since all the individual process steps are scalable, the process chain can be transferred to a plant scale, which in principle allows for commercial scale production. Nevertheless, this process for the spherical powder manufacturing requires high energy input and precise control of the process parameters in each step.

3.2. Solution-based methods

The solution-based methods, which include emulsion-evaporation and dissolution-precipitation, utilize surfactants and coupling agents to modify reinforcements and facilitate their blending with polymers in a solvent system. The composite powders can be obtained after solvent evaporation or filtration. The solution-based methods possess the advantages of improving surface affinity between fillers and polymer chains, enhancing the homogeneity of composite materials as well as forming spherical powders with good flowability.

3.2.1. Emulsion-evaporation

Emulsification is needed to mix monomers, oligomers or polymers with an emulsifier in an oiled system to create the emulsion water/oil system with the droplets in which polymerization and crosslinking are initiated by heating or radiation or in an enzymatic way (Fig. 6a to Fig. 7a). Fillers or additives are encapsulated by crosslinked polymer chains in the emulsion droplets to form composite microcapsules. Paggi et al. [151] and Wang et al. [121] reported that in an oil/water system, multi-walled CNTs and nanosilica were dispersed in the emulsion droplets of pre-polymer PA12 with the facilitation of chloroform. Zhou et al. [135] prepared composite microcapsules through dispersing the carbonated-HA nanoparticles and emulsifier PVA into the PLLA-dichloromethane solution. The solvents of these emulsion solutions can be easily evaporated. The obtained composite powders have desirable composition and morphology. However, the major drawbacks are the low productivity and the waste of organic solvents and emulsifiers.

3.2.2. Dissolution-precipitation

Dissolution-precipitation for powder preparation mainly relies on a thermal-induced phase separation of polymers in a solvent system. The reinforcements can be dispersed uniformly into a soluble polymer or pre-polymer matrix by ultrasonic oscillation or mechanical stirring under an elevated temperature [182]. The sol-

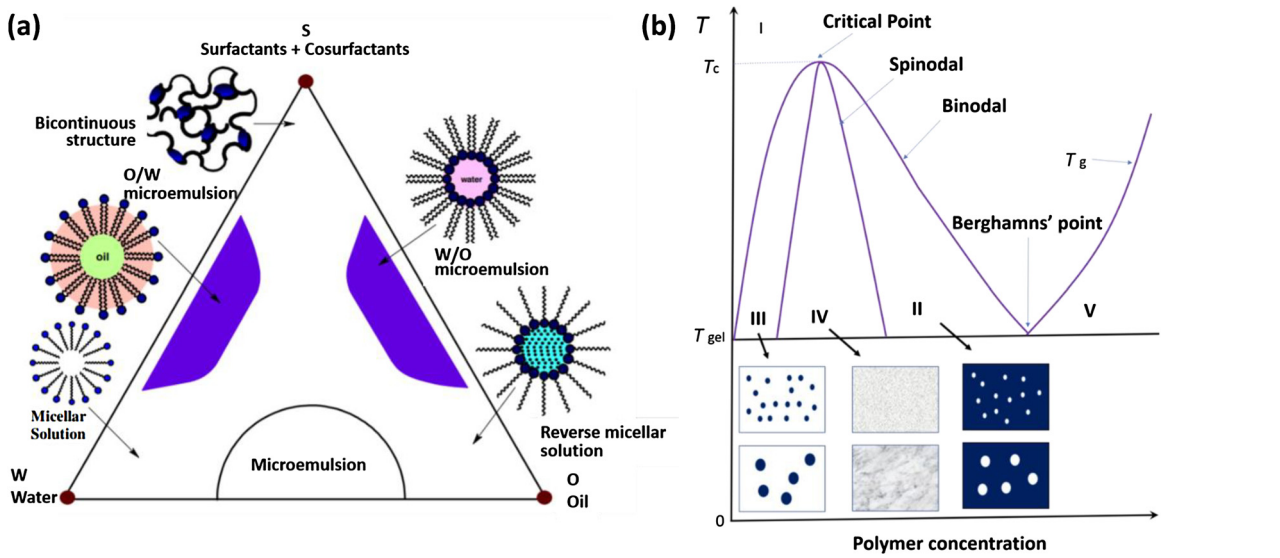

Fig. 7. Schematic illustrations of the physicochemical mechanisms of the solution-based methods: (a) emulsion-evaporation and (b) dissolution-precipitation. In (a), microemulsions are isotropic droplet mixture of oil, water and surfactant in which polymerization occurs and forms spherical powders. Typically, the direct emulsion (oil dispersed in water, o/w), reversed emulsion (water dispersed in oil, w/o) and bicontinuous structures are the three types of mixture configurations in the w/o/s mixtures. In (b), dissolution-precipitation is a thermal-induced phase inversion process in which the polymeric powders precipitate out from the solvent system once the polymer concentration is within the range of the spinodal phase and binodal phase.

ubility and phase separation of polymers are well controlled by the factors of polymer concentration, temperature and pressure (Fig. 7b). The spherical droplets of the polymer phase with fillers can be solidified and separated from the solvent phase upon cooling and complete precipitation. Lao et al. [33,78] and Chunze et al. [25] dispersed nanosilica and nano-TiO_2 into the PA12 phase in ethanol, respectively, and then the composite powders precipitated out after cooling. Shahzad et al. [114,119] mixed ceramic particles with polymer chains to obtain the polymer-functionalized composite powders such as Y_2O_3-ZrO_2/PP and Al_2O_3/PA12 for an indirect laser sintering process. This offers a solution to produce highly porous ceramic structures using a polymer as a removable binder

3.3. Spray drying

Spray drying is a physicochemical technique to apply high pressure on an atomizer nozzle to spray droplets of a polymer solution and instantaneously evaporate the solvent in order to obtain the microspheres of polymers or their composites [183,184]. The spray drying technique for powder manufacturing can be spraying polymeric powders in a gas phase at low temperature (spray freeze drying) or spraying the droplets into an antisolvent to maintain the initial geometries of the powders (Fig. 8). Mys et al. [185,186] successfully applied spray drying to obtain the microspheres of amorphous PS for usage in the SLS process. Nevertheless, in Fig. 7c to Fig. 8c, the rapid solidification of the polymeric phase and the fast evaporation of solvent generate invertible cavities or hollow structures within individual powders, and thus the spray-dried powders are usually irregular and exhibit high porosity and weak mechanical properties [186,187]. This powder manufacturing process is suitable for polymers such as PS, PLA, PLGA and PVP (Polyvinylpyrrolidone), as their products with inferior mechanical properties are acceptable for the industries of casting, biomedical engineering and food manufacturing.

3.4. Multiple-step methods

A multiple-step method includes not only a main powder manufacturing process, but also a pre-process or post-treatment process or both. In the pre-process, the preparation of bulk composites via melt-emulsion, melt-compounding or solution intercalation can conveniently encapsulate fillers in a polymeric matrix. A post-coating is to cover the powder surface with a layer of nanomaterials or organic additives, in order to modify the surface chemistry or limit electrostatic force for improved powder flowability.

3.4.1. Melt-emulsion with rotating shearing

Melt-emulsion is a top-down approach to melt and disperse the polymers or their composites in a continuous phase with emulsifiers at an elevated temperature. A shear or tensile force is then applied to the pre-emulsified droplets in a rotor to produce spherical microspheres with desirable size and size distribution, which are subsequently cooled and solidified in the large quantity (Fig. 9). Fanselow et al. [188] demonstrated the suitability of this two-step method to produce PE and PP powders in the continuous phases of water and hexadecane, respectively. The critical factors to control the powder morphology include the elevated temperature, the applied shear stress and shear rate, the mixing ratio of polymer and solvent phases, and the emulsifiers. In addition, the emulsifiers are required to be effective during the phase changes to ensure long-term stability against agglomeration. However, this process requires sufficiently high energy input for breakup of viscous droplets, stabilization against coalescence and scaling in reactors and pipes.

3.4.2. Melt-compounding with ball milling/spray drying

Melt-compounding applies mechanical forces to blend polymers or mix reinforcements with the melted polymers in a non-solvent condition, using a twin-screw extruder [79,159,160]. The physicochemical factors of material composition, functionalization, process temperature and pressure simultaneously influence the intercalated or exfoliated distribution of fillers in the polymeric matrix. These composites are then processed into powder forms by ball milling or spray drying. Wang et al [129] obtained the intercalated composites by blending nanoclays of rectorite and montmorillonite with the matrices of PA12, PA11 and PS. Paggi et al. [151] and Bourell et al. [18] prepared the exfoliated nanocomposites with carbon nanomaterials such as multi-walled CNTs and

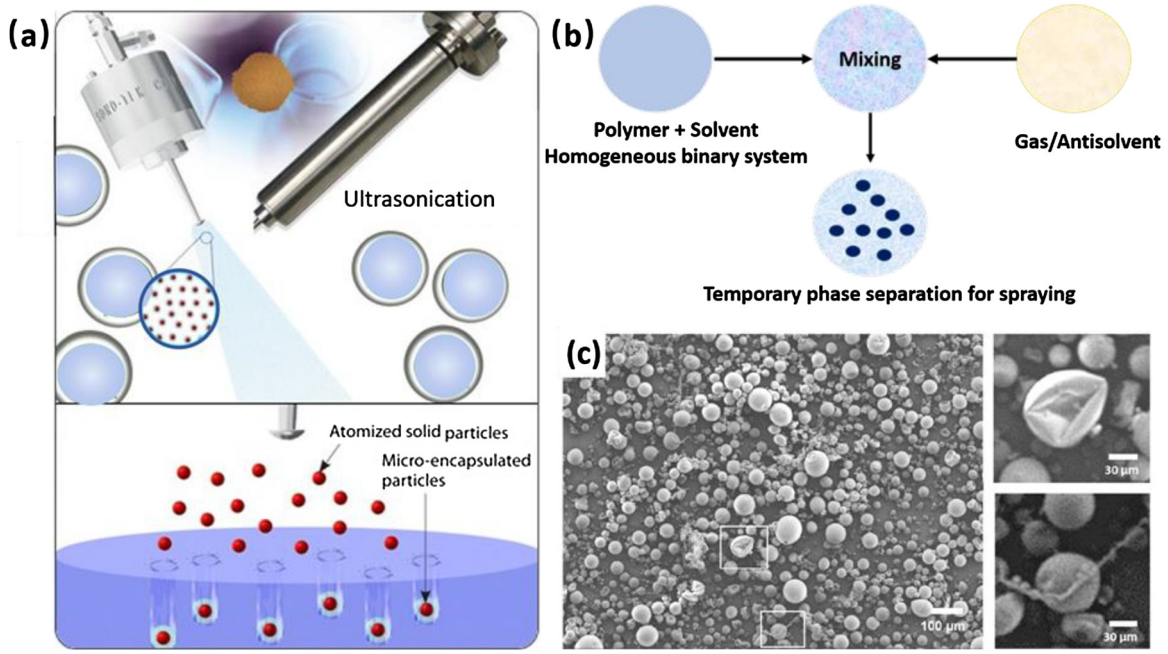

Fig. 8. (a) Illustration of the spray drying process to produce composite powders, (b) illustration of the droplet formation in a solvent/antisolvent system, and (c) the morphology of the free-flowing powders (e.g., polysulfone) produced by spray drying [185]. Copyright 2016 Reproduced with permission from MDPI AG.

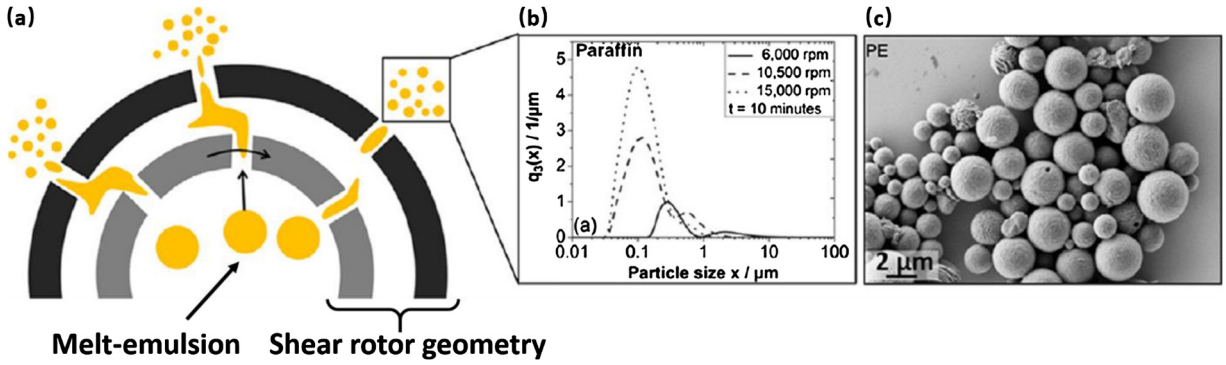

Fig. 9. (a) Schematic illustration of the process chamber for melt-emulsion with rotating shearing, (b) the rotational speed influencing the size distribution of powders, and (c) the produced spherical powders (e.g., PE) [188]. Copyright 2016 Adapted with permission from Elsevier Inc.

nanooxides such as Al_2O_3, FeO, CoO and Co_3O_4 for enhancing mechanical and fire-retardant properties simultaneously. However, this process is infeasible or challenging for polymers with high melt viscosity (e.g., PAEK family, aromatic PC, and PVC with high polarity), which requires extremely large shear force to embed fillers into the polymeric phases. The highly viscous flow of a melted polymer limits the total loading of the secondary constituent phase and may induce adverse and irreversible agglomerations [189].

3.4.3. Solution intercalation with ball milling/spray drying

Solution intercalation is employed to prepare exfoliated or intercalated nanoclays-reinforced polymeric composites through *in situ* synthesis or ultrasonication, which can assist polymer chains in adsorbing onto the interspaces among clay platelets in a solvent [190]. After being stirred constantly at an elevated temperature, the polymeric composites can precipitate out with a desirable distribution of fillers. The obtained bulk composites then undergo the vacuum drying and milling or grinding processes to form powders [191]. This two-step method is also available to disperse graphite/PMMA and graphite/PP in a chloroform and xylene system and then precipitate bulk composites for powder preparation [22]. The critical issue is the removal of residual solvents, which may cause adverse oxidation of polymers in the thermal fusion process.

3.4.4. Single-step method with post-coating

A post-coating process can be applied to core powders manufactured from a single-step method previously discussed. One type of process is to coat polymeric materials on the surfaces of powders which are intractable materials of oxides, carbon fillers, ceramics and metals [106]. In the powder-based fusion, coated polymer layers behave as binders to glue the core materials, and their green parts with complex geometries can be obtained after the removal of the polymeric phase [106,114,116]. The other type is to cover the surface of polymeric powders with nanomaterials, which can absorb onto the polymer surface due to strong van der Waals forces and chemical interactions. The coated nanoparticle layer is capable of improving flowability and processability of powders and extending the functionality of printed products. For instance, CNTs-coated PA12 powders exhibit improved flowability and laser energy absorption capability [60,71,187].

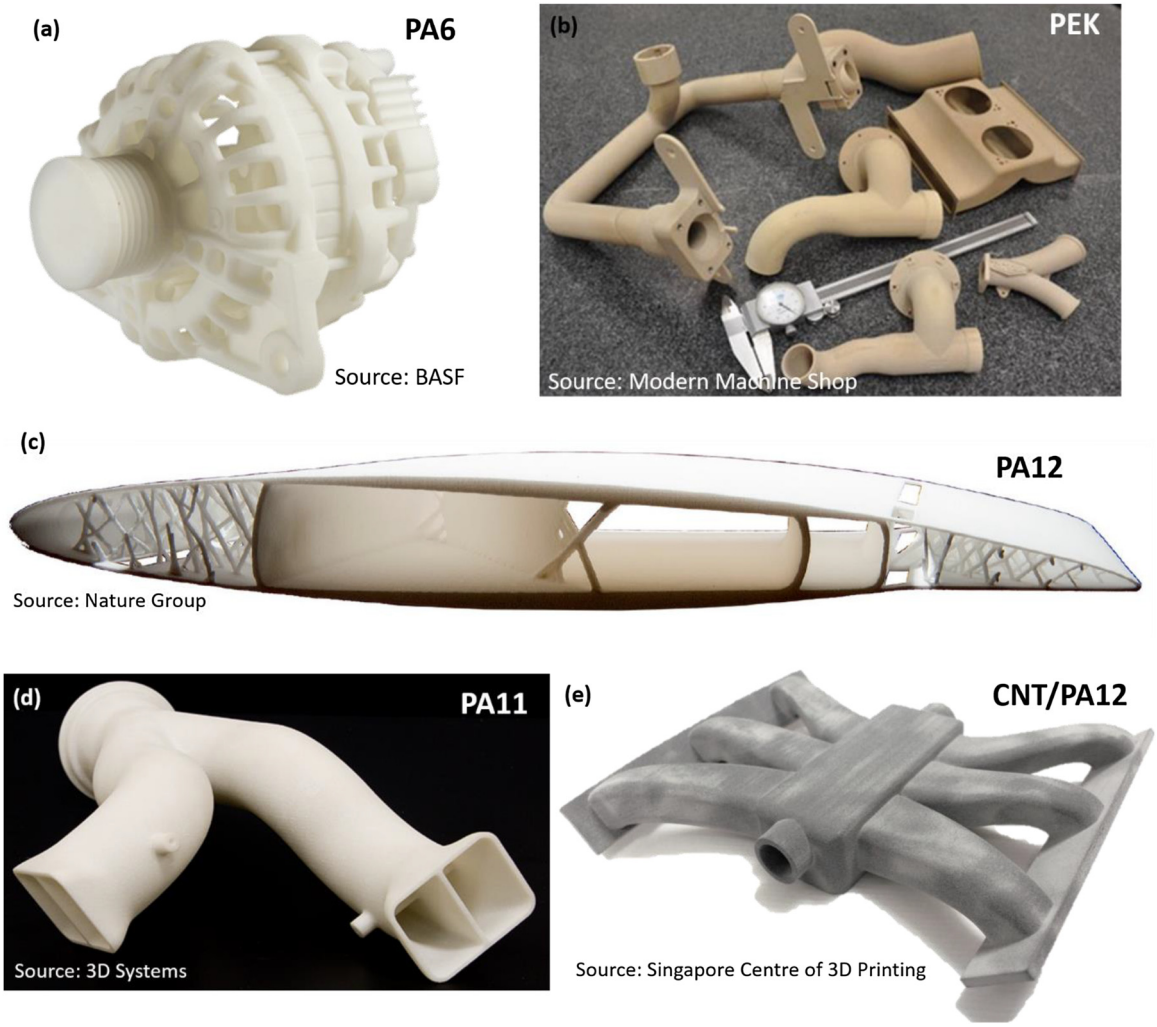

Fig. 10. (a) Automotive components of PA6 manufactured by laser sintering from BASF Group; (b) the laser-sintered PEK components via air pipes; (c) the optimized full-wing structure fabricated by a powder-based AM technique [198]. (d) the airduct of PA11 fabricated by SLS, and (e) automobile inlet manifold model of laser-sintered CNT/PA12 composites [199]. Copyright 2017 Reproduced with permission from Nature group, Copyright 2018 Reproduced with permission from Elsevier Inc.

4. Properties and applications

AM techniques offer novel strategies to achieve a systematic integration of material selection, design principle and manufacturing freedom, resulting in the ease of fabrication of main components or entire devices and equipment for functional applications [52]. This section presents the properties and functionalities of printed products and their various intriguing applications as well as future trends to address and discuss open issues and potential research directions in material development and structural design.

4.1. Automotive, aerospace and military

It has gained intensive interest to develop high-performance polymers and their composites for powder-based AM to fabricate light-weight and robust components with complex geometries in order to meet stringent requirements in automobile, aerospace and military applications [192,193]. The reinforcements in printable composites enable them to possess multi-functionalities such as mechanical, thermal and electrical properties.

4.1.1. Mechanical components

Engineering polymers and their composites printable by AM are fast gaining ground as favourable materials for construction of automobile, aircraft and spacecraft (Fig. 10). The integrated requirements of structural components for aerospace or automobile focus on lightweight, superior mechanical strength and modulus, high fatigue resistance, high impact damage resistance, etc. Since few polymers except high-performance ones can satisfy such stringent mechanical requirements, an emerging group of reinforcements via short carbon fibers and carbon nanomaterials were proposed to reinforce polymers for structural applications [190,194]. Nevertheless, printed polymeric composites have such problems as poor impact damage resistance, weak fatigue resistance and anisotropic mechanical properties due to the presence of micropores or nanopores, poor interfacial adhesion between polymers and fillers as well as the anisotropic microstructures along different building directions.

The high-performance polymers of PAEKs family possess the outstanding mechanical performances including good specific strength, excellent thermal stability and resistance to creep and fatigue. PAEKs and their composites have large potential to replace inferior aluminum alloys for lightweight vehicles and aircraft [82]. As shown in Fig. 10b, PEK has the advantageous service temperature up to 260 °C and thus it is employed to fabricate the airpipes or airducts with complex geometry satisfying the stringent temperature requirements in aerospace. Recently, Yan et al. [195] employed the CFs with high aspect ratio to reinforce the PEEK matrix dur-

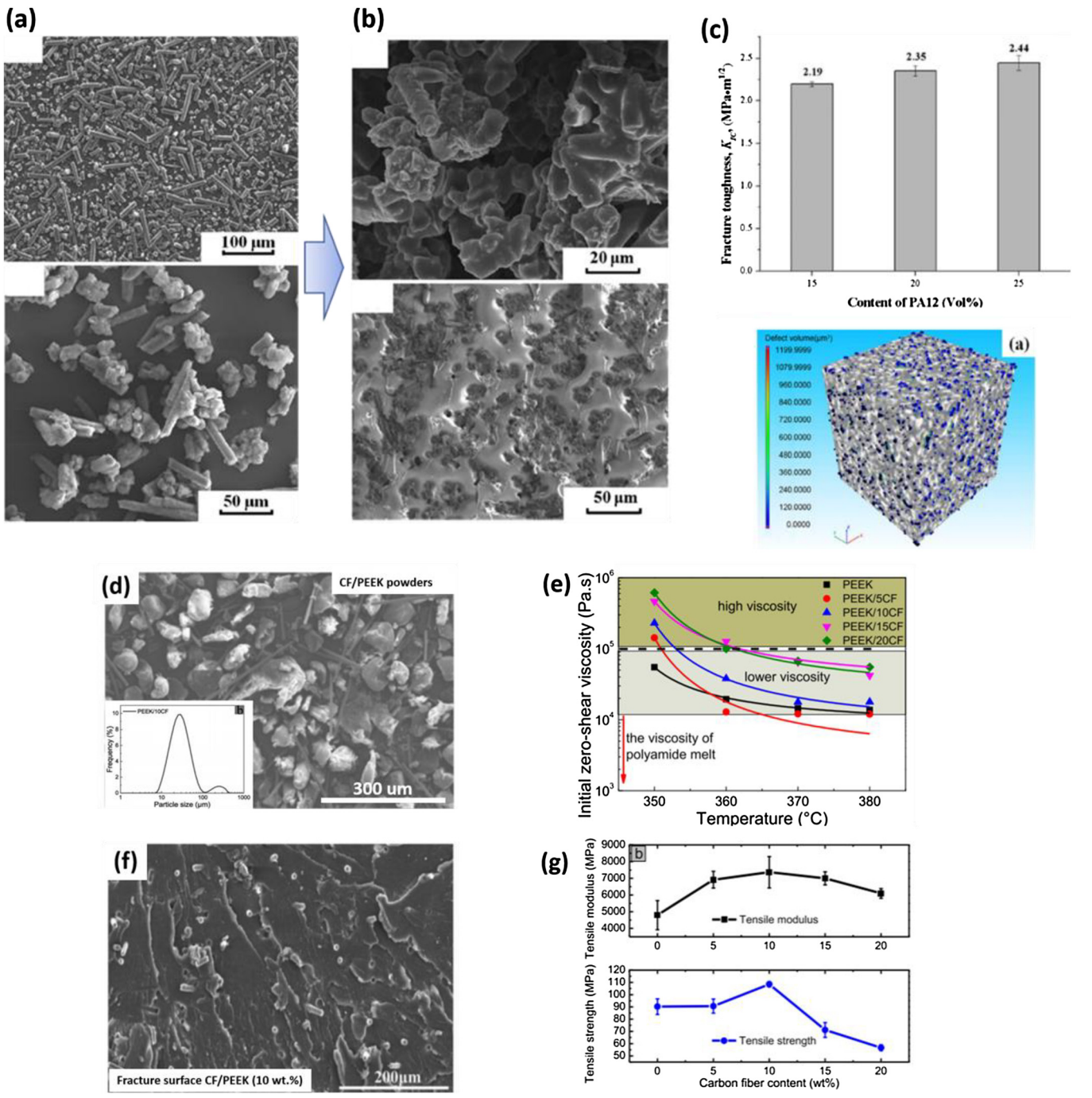

Fig. 11. (a) Short carbon fibers coated with PA12; (b) microstructures of the CF/PA12/Epoxy composite fabricated through laser sintering of CF/PA12 and infiltration of epoxy; (c) diagram of fracture toughness versus PA12 composition, together with the image of the filler and polymer distributions by micro-CT (computed tomography) scanning [153]. (d) the morphologies of CF/PEEK powders; (e) melt viscosity of CF/PEEK composites with varied CF loading ratio; (f) the fractured surface of CF/PEEK (10 wt%) perpendicular to the direction of fiber alignment; (g) the tensile properties of sintered composites with different CF loading ratio [195]. Copyright 2015. Adapted with permission from Nature Group. Copyright 2018. Adapted with permission from Elsevier Inc.

ing laser sintering, and the optimized CF/PEEK (10 wt%) composite exhibited excellent tensile strength of 109 MPa and Young's modulus of 7 GPa along the direction of fiber alignment (Fig. 11d–g). However, the anisotropic mechanical performance is undesirable for the lightweight component development in aerospace or military. Advanced laser material Inn. developed a type of CF/PEKK composite powders, in which the short carbon fibers were encapsulated by PEKK matrix through ball milling. The laser-sintered composites exhibited the isotropic enhancements of the mechanical modulus and strength [155,194]. In recent years, the company EOS has fabricated lightweight components of CF/PEKK via SLS for aircraft manufacturing in Boeing and Airbus. The encapsulation of fillers within powders could overcome the drawback of anisotropic mechanical properties of composites caused by the prior orientated packing of fillers upon powder deposition [157,196,197]. The recyclability of carbon fiber/PEKK powders (up to 60%) was significantly improved, compared with previously available PEK powders in commercial market [67,88,95].

Other engineering polymers such as PP, PA6 and PA12 and their composites have been used to print various vehicle components

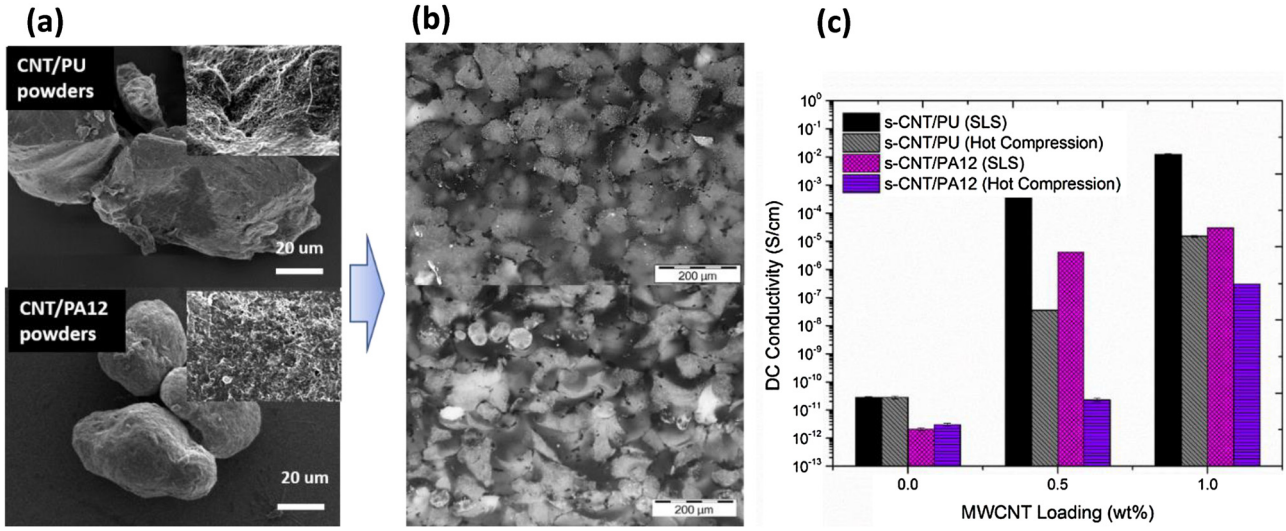

Fig. 12. (a) PA12 and PU powders coated with CNTs; (b) microstructures of SLS-printed CNT/PA12 composites; (c) electrical conductivities of CNT/PA12 and CNT/PU composites manufactured by SLS and hot compression [199]. Copyright 2018. Adapted with permission from Elsevier Inc.

including battery covers, air conditioning ducts and functional mounting brackets (Fig. 10) [79]. Intensive research works have been devoted to powder evaluation and process optimization to improve the performances of products printed from these materials [26,153]. Zhu et al. [68] reported that the printed PP parts exhibit a low degree of crystallinity and possess the comparable tensile strength the injection moulded PP components, but the elongation at break of printed PP parts scarified under 5%. Recently, BASF Group has partnered with Farsoon Hi-tech to develop printable PA6, and their laser-sintered products exhibited higher service temperature and greater mechanical strength than those of other PAs [79].

Moreover, the advanced mechanical performances of polymers can be enabled by carbon nanomaterial reinforcements such as CNTs and short carbon fibres. Bai et al. [60,71,200,61,201,212] reported that the CNTs-coated PA12 and PA11 powders could be processed by SLS, resulting in embedded-CNTs that toughened and strengthened the polymeric matrices simultaneously. Further, Yuan et al. [199] demonstrated 3D auxetic metamaterials via CNT/PA12 with great potential for the applications in impact protection and cushion. Zhu et al. [152] reported a novel approach to prepare the high-performance carbon fiber/PA12/Epoxy composites through laser-sintering process and post-infiltration (Fig. 11). The resulted composites yielded much higher isotropic properties of ultimate tensile strength (101.03 MPa) and flexural strength (153.43 MPa) than other reported SLS products.

4.1.2. Electrical and magnetic usages

As neat polymers are usually electrical insulators, intensive interest has been drawn to developing electrically conductive composites to ensure electrostatic charge dissipation and even further to allow current flow through the structures. Carbon fibers, carbon black, CNTs and graphite pellets have been blended with polymers to achieve composite materials with electrical conductivity of 1–10 S/m, as required for antistatic applications. Athreya et al. [43] firstly reported that the laser-sintered carbon black/PA12 parts exhibited much higher electrical conductivity than injection-moulded ones, However, the conductive carbon black/PA12 exhibited significant reductions in the mechanical strength and elongation at break, compared with PA12.

Recently, Yuan et al. [199] developed CNTs-coated PA12 and TPU powders for laser sintering to achieve nanocomposites with segregated conductive CNT networks as shown in Fig. 12. These composites exhibited enhanced electrical and mechanical properties simultaneously. Especially, the laser-sintered CNT/TPU retained the high flexibility and durability of an elastomeric polymer and functioned as a mechanical responsive conductor.

Nowadays it is crucial to avoid the emerging hazards of electromagnetic radiation on human health and stability of electrical equipment due to the usage of wireless communication and microwave devices. Microwave absorption materials such as magnetic and electrical dampers offer an effective method to solve the issue by converting the electromagnetic energy to thermal energy or dissipating it by electromagnetic damping. Conventional magnetic materials such as Fe, Ni, Co and their alloys ranging from the nanometer to micrometer scale can be incorporated with the polymeric matrix for powder-based AM. Recently, carbon-based materials including SiC, CNTs and graphene-reinforced polymers were reported to possess the capability of anti-electromagnetic interference (EMI) and absorb electromagnetic waves in the gigahertz range [201–203]. Therefore, the incorporation of microwave absorbers with polymeric powders will open an avenue to direct manufacture of functional components for EMI shielding.

4.1.3. Flame-retardancy and thermal conduction

Another aerospace-driven need is to focus on flame-retardant polymers and polymeric composites. The inherent flame retardancy and high operation temperature (>260 °C) make PAEKs suitable for high-end functional components such as air ducts and exhausts as well as highly customized interior parts for aircraft. Nevertheless, high-performance polymers are cost-prohibitive for the industries requiring mass production. Other engineering polymers are usually derived from fossil fuel-based hydrocarbon feedstocks and thus are highly flammable. Therefore, polymeric nanocomposites become attractive as they are capable of withstanding both thermal and mechanical impact loading.

Three types of additives have been introduced to reinforce the flame-retardant performance of polymers: nanofillers such as nanoclays, nanosilica and polyhedral oligomeric silsesquioxane [204]; nanofillers such as carbon nanofibers, CNTs and graphite [154]; flame-retardant additives such as phosphorous/nitrogen-based compounds [205–207]. Lao et al. [33] investigated the fire-retardant performances of laser-sintered PA12 and PA11 with the addition of CNTs, carbon nanofibers, nanoclays and intumescent additives. During ablation, the intumescent additives and carbon nanofibers induced a synergetic mechanism to prohibit fire initiation and form char layers for controlling the heat release rate.

Moreover, nano-additives such CNTs and nanoclays could improve thermal insulation and reduce mass loss because they could re-emit the incident heat radiation to the gas phase from the char layers and then minimize heat transfer to the inner matrix [31,208]. Tungsten (W), SiC and carbon fiber-reinforced composites with high thermal stability and mechanical modulus can be prepared by indirect laser sintering. For instance, the carbon/carbon composites were recently manufactured by laser sintering and post-degreasing process and demonstrated good thermal stability for the usage requiring high-service temperature [209]. Thermal conductivity is another critical property of materials, which influences their applications in aviation, aerospace and automobile industries. Conventionally, polymers are known as thermal insulative materials, and many research works have been conducted to develop thermally conductive polymers or their composites [28,109,210–215]. However, the composites via powder-based AM have not exhibited significant improvement on thermal conductivity, compared with neat polymers. This is mainly because the weak affinities at polymer-fiber and fiber-fiber interfaces and the presence of micropores can cause phonon scattering and limit phonon propagation among the matrix. In order to overcome this process-induced drawback, the surface functionalization, hybridization and encapsulation of thermally conductive fillers in the stage of powder preparation may provide a solution to further enhance interfacial affinities, thus promoting thermal conduction.

4.1.4. Future trends

With the advances of machine and software development, it is worthwhile devoting efforts to feeding materials via polymeric composites with new compositions and controllable configurations. High-performance polymers and their composites are an emerging class of materials due to their capability of withstanding thermal and mechanical loading at the same time. Various nanoparticles such as nanosilica and nanoclays with surface functionalization can be added in polymers to act as thermal insulative elements for improving the integrity and toughness of char layers and contributes to the mechanical performance of polymeric matrices. Owing to the multi-functionalities of carbon materials, carbon/polymer, carbon/carbon and carbon/ceramic composites via direct and indirect laser processes are expected to have superior performances in electrostatic and EMI shielding, oxidation resistance, ablation resistance, thermal shock resistance, and high-temperature impact loading resistance.

In structural design, multi-physics and parametric topological optimization extends the possibility of optimum design to achieve the lightweight, mechanical strengthening, damping and impact resistance of AM products. It is challenging for lightweight composite structures to withstand dynamic or cyclic compressive loading, and therefore their stress-intensive regions such as thin walls and frame connection nodes need to be further configured for toughening. The thermo-mechanical coupling effects on the properties of materials and structures are open to discussion in the 3D topological evaluation [216]. Furthermore, smart polymers with shape memory or self-healing effects offer new possibilities in four-dimensional (4D) printing, which realizes the dynamic reconfiguration of the printed 3D structures in response to external thermal or magnetic stimulus. Therefore, reconfigurable and healable polymeric composites possess unique dynamic responses that have great potentials in the topological design field.

4.2. Healthcare and biomedical engineering

Intensive research works have been devoted into customized applications in healthcare and biomedical engineering. This section focuses on the application of anatomical models, prosthetics, tissue engineering, bio-implants, drug and therapeutic agent delivery.

4.2.1. Anatomical models and prosthesis

AM has been implemented not only for rapid prototyping but also for manufacturing personalized anatomical models (e.g., hearing aid casings, orthodontic brackets and surgical models) as well as prosthetic implants (e.g., hip prosthesis) [1,217,218]. With the development of tomographic techniques, 3D medical imaging techniques such as X-ray-based CT, magnetic resonance imaging (MRI) and positron emission tomography (PET) the reconstruction software tools have been coupled to obtain accurate personal 3D data and convert these data to visualized and printable models [218,219]. The advanced medical imaging and AM techniques are able to assist pathology diagnosis, support surgical training and planning for hip, knee or shoulder operations, and improve the efficiency and precision of these operations [220–224]. For example, Leiggener et al. [225] used the Surgicase-CMF software to simulate surgery on a workstation and guide the SLS system to facilitate the osteotomy and osteosynthesis to be performed with intact circulation during surgery on the fibula. Apart from stiff PAs, soft elastomers TPE and TPU have been used to build the vascular structures, the flexible mitral valve models, and the entire heart and stomach models with internally connected inner chambers [226,227].

4.2.2. Tissue engineering and bio-implants

Tissue engineering is an interdisciplinary field integrating areas of cell biology, materials science and engineering, and clinical study toward the development of alternative tissue structures that restore, heal and improve the normal tissue and organ function [228,229]. Biopolymer composites are of great interest in tissue engineering because they offer a favorable environment for the growth and differentiation of cells [140,230,231]. Powder-based processes such as SLS and binder jetting are effective techniques to create polymeric composite materials with interconnected networks of micropores mimicking the native *in vivo* topographic features of the extracellular matrix (ECM) [40]. Especially, hard-tissue engineering such as bone and cartilage repair needs tissue scaffolds to provide an ECM which facilitates cell attachment, proliferation and differentiation and allows cell delivery and retention in an appropriate biomechanical environment for tissue regeneration. The selection of materials depends on the types and properties of tissues to be replaced or regenerated as well as the duration of regeneration.

One advantage of powder-based AM processes is to control the hierarchical porosity and mechanical properties of scaffolds with complex design and low cost. Chua et al. [232–234] proposed a group of polyhedral functionally graded scaffolds and provided the correlation between the scaffold porosity and compressive stiffness (Fig. 13a). The pre-designed scaffolds need to be evaluated by mechanical modeling and testing to achieve a desirable range of mechanical properties before being adapted into the *in vivo* and *in vitro* environments [104,235].

Various bio-polymers and their composites are available for hard-tissue scaffolds and bio-implants that can be personalized and digitalized [10]. Laser-sintered PEEK parts with graded porous patterns were investigated as bone replacements due to their excellent mechanical performance, chemical stability and biocompatibility [180,196,236]. Other biopolymers, especially PLA and PCL, allow the fabrication of porous scaffolds for the engineering of cell attachment, growth and proliferation [141,144]. In the binder jetting system, the mesoporous scaffold of PLGA can be achieved by using chloroform to bind NaCl/PLGA powders and then immersing the product in water to leach out the salt [237,238]. However, hydrophobic polymers (e.g., PCL) have poor interactions between the polymer matrix and cells, thus limiting cellular adhesion and growth [239]. The inferior mechanical strength, toughness and fatigue resistance of PCL, PVA and PLA scaffolds restrict their

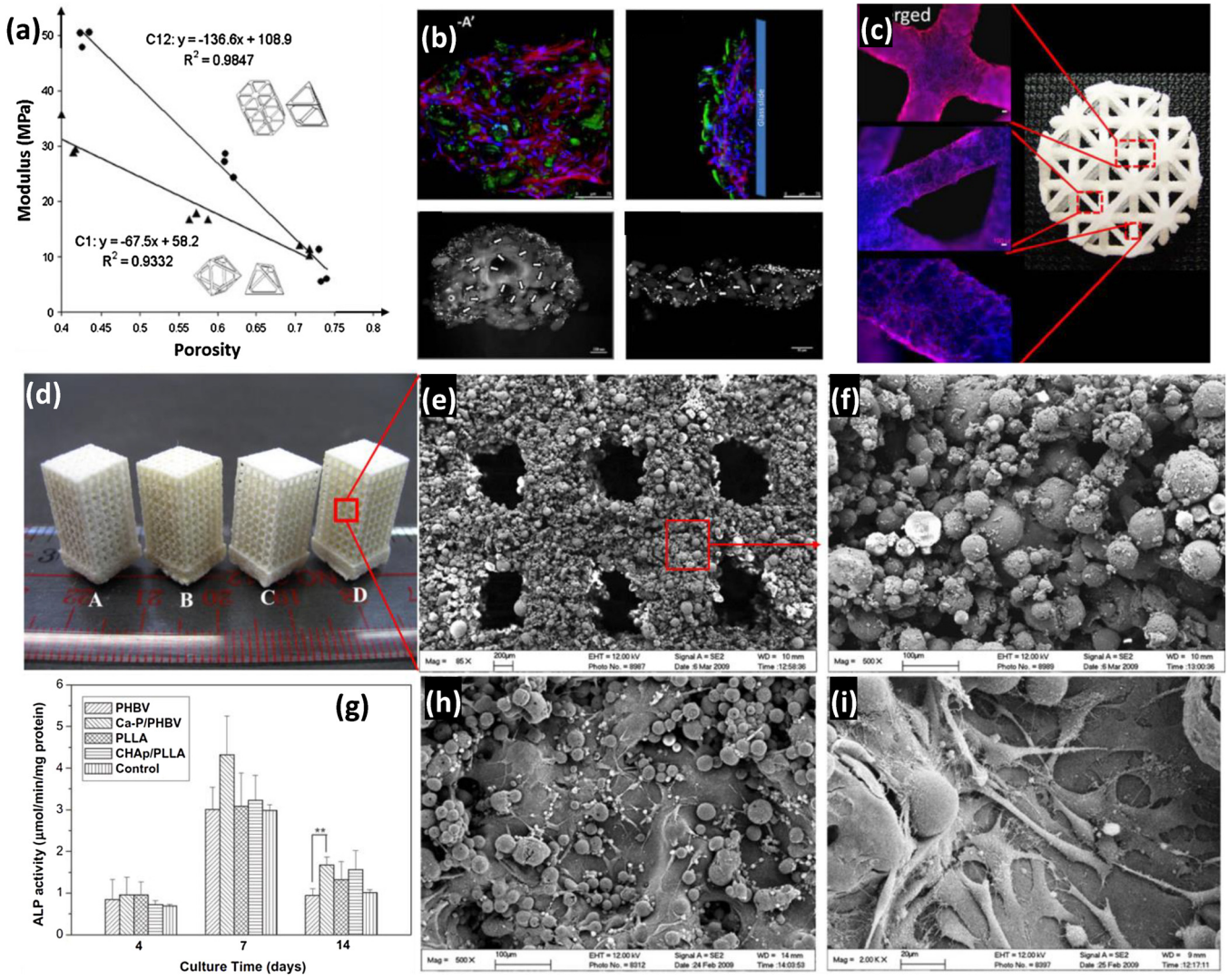

Fig. 13. Tissue scaffolds and bio-implants fabricated by powder-based AM: (a) modulus versus porosity of the graded porous scaffold [232]; Copyright 2011. Adapted with permission from Elsevier Inc. (b) florescent optical images of cell attachments on the printed scaffold in an *in vivo* environment; (c) florescent optical characterization of a truss scaffold at various locations [104]. Copyright 2010. Adapted with permission from Elsevier Inc. (d) Demonstration of various types of graded porous scaffolds; (e) and (f) scanning electron microscope (SEM) images of the HA/PCL scaffold with different magnifications; (g) bioactivities of different scaffolds over culture time; (h) and (i) SEM images of cell attachments and propagation on the Ca-P/PHBV [136]. Copyright 2014. Adapted with permission from Elsevier Inc.

use for bone replacement applications [149,240,241]. Furthermore, the degradation procedures of PLLA, PLAGA and PLGA are random and bulky hydrolysis of ester bonds in the polymer chain and possibly cause premature failure of the scaffold [242–244]. In addition, the release of acidic degradation products can cause a strong inflammable *in vivo* response. The degradation kinetics are influenced by several factors including porosity, chemical composition, geometric structure, material phase of scaffold (crystalline, semi-crystalline and amorphous), polydispersity of polymer, the presence of additives and hydrophobicity [50,88,244].

An incorporation of bio-ceramics with polymer matrices has been investigated to improve the performance of bone substitutes through tailoring the degradation kinetics and enhancing the osteoconducitivity [244]. Bio-ceramics such as calcium phosphates (CaPs) and bioglasses such as SrO, CaO, ZnO and P_2O_5 have demonstrated high compatibility and bioactivity within the *in vivo* and *in vitro* environments [109,245], which enable improvements in density, phase stability and biodegradability of the composite scaffolds [245,246]. CaPs are a group of ceramic materials that exhibit significant differences in physical, mechanical and biological properties, and are typically used for bone and teeth tissue replacements because of its similar composition with natural bone and teeth [26]. For instance, HA ($Ca_{10}(PO_4)_6(OH)_2$) contains a favourable compositional ratio of Ca/P (close to 1.67), which is found in natural tissues such as bones. Duan et al. [136] and Xia et al. [139] employed SLS to fabricate scaffolds using HA/PLLA and HA/PCL composites, which possess hydrophilicity and high roughness at the internal surface of scaffold pores and channels. As shown in Fig. 13f, it was observed that *in vitro* osteoblasts were tightly anchored to the surface of the nano-HA/PCL scaffold and exhibited fibroblast-like morphology after a 12-hour culture; *in vivo* active bone regeneration was found at the interface of the ceramic phase and bone, showing good osteoconduction with the implantation of HA nanoparticles.

Tricalcium phosphate β-TCP is another popular CaP material applied to enhance the biodegradability and dissolution kinetics of composite scaffolds, as it shows an increased biodegradation rate compared to HA [110,146,148]. Wiltfang et al. [243] investigated TCP as a biodegradable filling material in the defects of the tibiae head of minipigs. The β-TCP and HA can selectively trigger integrin receptors and promote differentiation of cells into newly formed trabeculae. Simultaneously, the osteoclasts resorbed the materials by dissolution of bio-ceramic particles and the newly pro-

duced collagen replaced the degraded organic matrix [143]. PLLA composites such as β -TCP/PLLA exhibit a high specific modulus, fracture toughness and strength-to-weight ratio as compared with the pure β -TCP components [145]. Khang et al. [230] also found that the nanoceramics on the scaffold surface of the Ca-P/PHBV composite could promote the attachment, growth and differentiation of osteoblasts, and this composite scaffold showed relatively high bioactivities as compared with other scaffolds (Fig. 13g–i). Therefore, bio-ceramics-reinforced polymers are promising composites for the development of biodegradable implants and bone tissue engineering [247,248].

4.2.3. Drug and therapeutic agent delivery

Drug and therapeutic agent delivery usually require predetermined drug release profiles that ensure optimal release rates and absorption of the drug to improve its efficacy and safety, particularly in the areas of targeted and controlled delivery [249,250]. The driving factor for such an application is its capability of engineering the release profiles by controlled spatial distribution with customizable composition of polymers, drugs and other additives [250,251].

Biodegradable implants and drug carriers have also been fabricated for operations and treatments. For instance, the TCP/PLGA scaffolds were printed with anti-tuberculosis drugs embedded into its support structures. *In vivo* response, the drugs released stably and were found to be efficient against tuberculosis-causing bacteria. The degradable scaffold induced effective migration and survival of rat bone marrow mesenchymal stem cells, resulting in successful bone regrowth and repair [251]. Through binder jetting, the drugs or therapeutic agents can either be digitally sprayed onto the powders or incorporated with the powders prior to controlled particle fusion [252,253]. The various combinations of binders and powders for drug manufacturing were reviewed by Goole and Amighi [253]. Nevertheless, the study lacks a good understanding of the effects of carrier geometry on drug release, temperature limitation of drug printing and the release kinetics in current stages.

4.2.4. Future trends

Several issues involving hard tissue engineering still remain a challenge. The mechanical performance of scaffolds needs to mimic native-tissue behaviour, which has a hierarchical structure from nano- to macro-scale, combining linear and nonlinear elastic behaviours. Functional scaffolds with both structural and compositional variations can be fabricated for tissue engineering as AM can potentially minimize assembly requirements by manufacturing parts with multiple compositions.

Other critical issues in the end-use applications are the inherent concerns related to reliability and reproducibility of products, and the inflammatory responses due to the release of side products of polymer degradation. Most importantly, it is necessary for the underlying mechanism of cell generation and propagation to be comprehensively investigated through the interdisciplinary collaboration of biology, material science and manufacturing techniques. Recently, there is a new trend of employing 3D bio-printing to create artificial biological products using live cells, scaffold materials and extracellular matrices. Biological methods are also applied to guide cell generation, differentiation and tissue growth for simple functional organ formation based on mechanical and geometrical scaffold fabrication techniques.

In another aspect, AM has the potential to produce excellent bio-compatible vessels for targeted drug delivery. The digitalized deposition of materials offers the opportunity to fabricate drug carriers with desirable graded composition of drugs [254]. The kinetics of drug release can then be controlled by programming drug formulation and engineering carrier geometries instantaneously, which is a promising field for advanced drug delivery systems.

4.3. Water treatment and energy generation

Currently, available powder-based AM can be additionally applied to low-carbon manufacturing techniques in energy storage and environmental industries due to its capabilities of coupling with advanced nanotechnologies [255–258]. The applications in water treatment and energy generation are discussed in this section.

4.3.1. Water treatment and purification

3D structures can serve as a platform for all kinds of emerging environmental applications, particularly in the biofilm reactor [259] and membrane module components for removal or separation of pollutants and contaminants from liquid and gaseous environments such as spacers and filtration membranes [260–262].

In the membrane separation system, free channel spacers within a module are critical for facilitating recirculation of the bulk fluid and the fluid close to the membrane surface. As shown in Fig. 14c, printed novel spacers can effectively increase the local shear rate and fluid velocity, thereby minimizing the concentrated polarization effect by enhancing the mass transfer [263,264]. Recently, Tan et al. [260,261] investigated the geometric accuracy of benchmarked parts manufactured by SLS, FDM and PolyJet so as to guide the feature design of spacers as well as to ensure the model accuracy. Li et al. [264] fabricated the novel spacers with multi-layer twisted-structures and validated the enhanced performance of mass transfer for the membrane separation system. Thus, 3D-printed spacers with desirable geometric complexity can effectively promote water flow, provide sufficient mechanical support, and minimize the interfacial contact between spacers and membranes.

Bio-film reactors with moving beds are typical devices used in wastewater treatment, and bio-carriers are key components for enriching microorganisms and improving the amount of biomass in the reactor (Fig. 14e). Dong et al. [265] reported a group of laser-sintered bio-carriers with fullerene-like structures, which displayed effective microbial activity and adhesive ability for bio-film growth due to their high surface roughness and large surface-to-volume ratio as compared with hot moulded biocarriers (Fig. 14f). Tan et al. [261] observed that the spatial spacers produced via SLS possessed high surface roughness and showed relatively strong bacteria adhesion.

However, there are several limitations in the preparation of membranes for the filtration of pollutants and contaminants at the sub-microscale [261,266]. Resolution and scale constraints during printing restrict the fabrication of nanoporous structures used for water and gas separation applications. Several types of polymers such as PP and PA12 have been developed for the membrane module, but numerous candidate polymers and their composites are yet to be investigated [266,267]. Another drawback is that the cost of AM techniques is not comparable with that of conventional phase inversion-based methods [268–270].

4.3.2. Energy storage and generation

Components in energy storage devices including supercapacitors, batteries, solar cells and piezoelectrical parts can be fabricated with advanced materials such as graphene, CNTs, Mo_2S and TiO_2 using AM techniques [133,258,271]. As shown in Fig. 15, Azhari et al. [271] printed graphene-based composite electrodes via binder jetting for high-performance supercapacitors. The thermal-reduced graphene oxide was glued layer-by-layer using a minimal binder, and palladium nanoparticles were then impregnated into the porous graphene structures to improve the contact resistance. In addition, a nano-TiO_2 particle film was selectively sintered by near-infrared laser on a conductive plastic substrate to form elec-

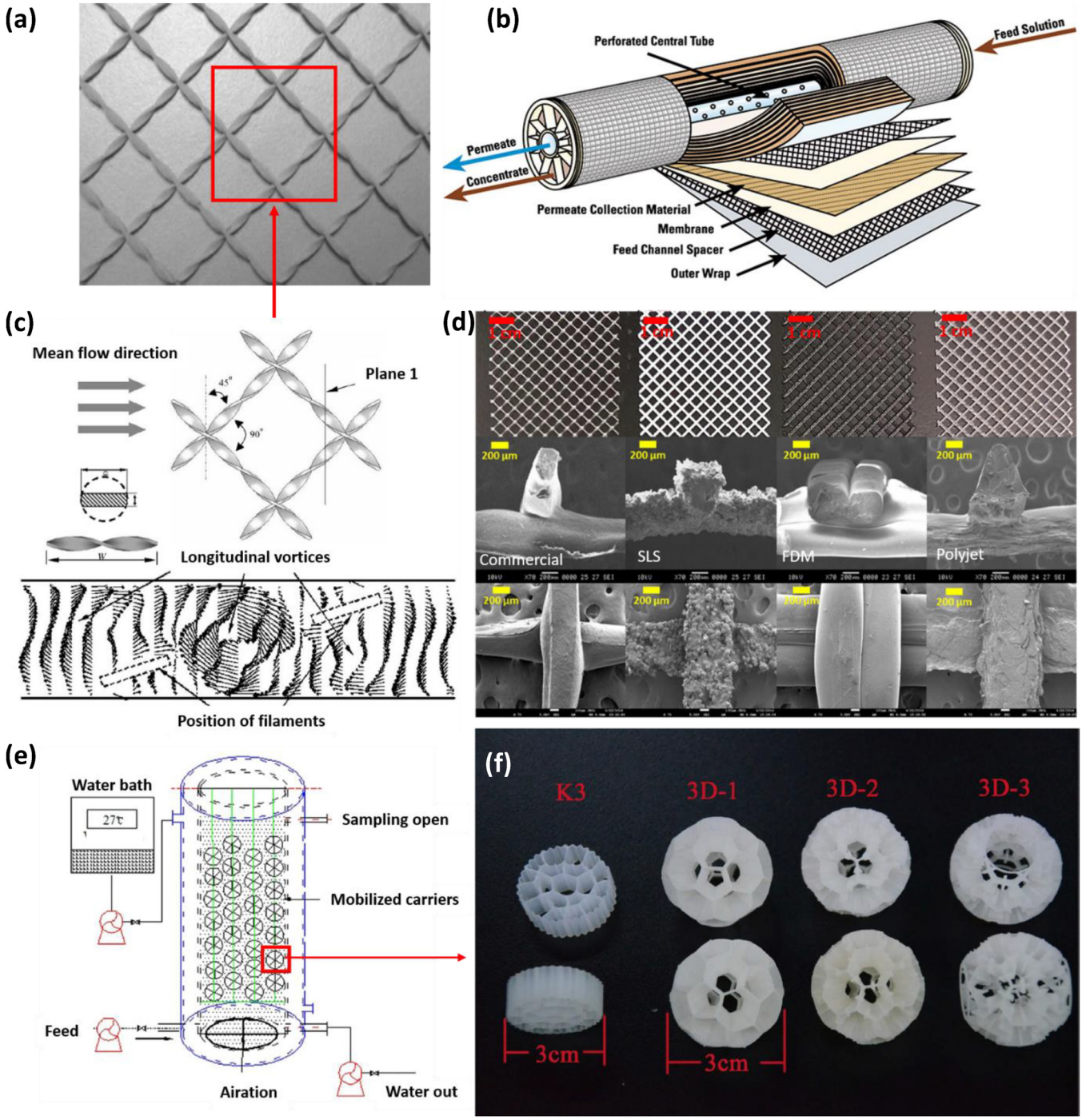

Fig. 14. (a) Novel spacer design fabricated by SLS; (b) integrated membrane modules of water treatment with laminated structures; (c) longitudinal vortices in a flat channel filled with spacers and the vector plot of velocities in Plane 1 [264]. (d) Photos and SEM images of spacers fabricated by the conventional process, SLS, FDM and Polyjet [261]; (e) schematic of the sequencing biofilm batch reactor containing different types of bio-carriers; (f) 3D fullerene-type biocarriers used in the bioreactor [265]. Copyright 2005 Reproduced with permission from Elsevier Inc. Copyright 2017 Adapted with permission from Elsevier Inc. Copyright 2016 Reproduced with permission from Nature group.

trodes for highly efficient dye-sensitized solar cells [133]. Laser energy can effectively and precisely promote electrical contact among nanoparticles and eliminate thermal damage of the plastic substrate, resulting in improved efficiency of charge accumulation. However, this particle sintering process based on thin-film coating is lacking systematic and automatic 3D control. Thus, the advantages of 3D structural flexibility have not been explored.

Nanocomposites used for harvesting mechanical and electrical energy such as nano-$BaTiO_3$/PA11 via SLS exhibit frequency-dependent dielectric properties that are required by piezoelectrical devices [121]. Nevertheless, the widespread use of AM techniques incorporating nanomaterials, especially in large-scale manufacturing, is still hampered by limited machine capabilities for material digitalization and automatic structural optimization. Therefore, it is a challenge to manipulate porous material structures in the meso- and nano-scale regime. Currently, the 3D-printed structures offer limited residential sets for charge carriers, and thus the printed composite anodes and cathodes possess inferior energy density, capacity and efficiency as compared with composites produced from conventional nanofabrication techniques.

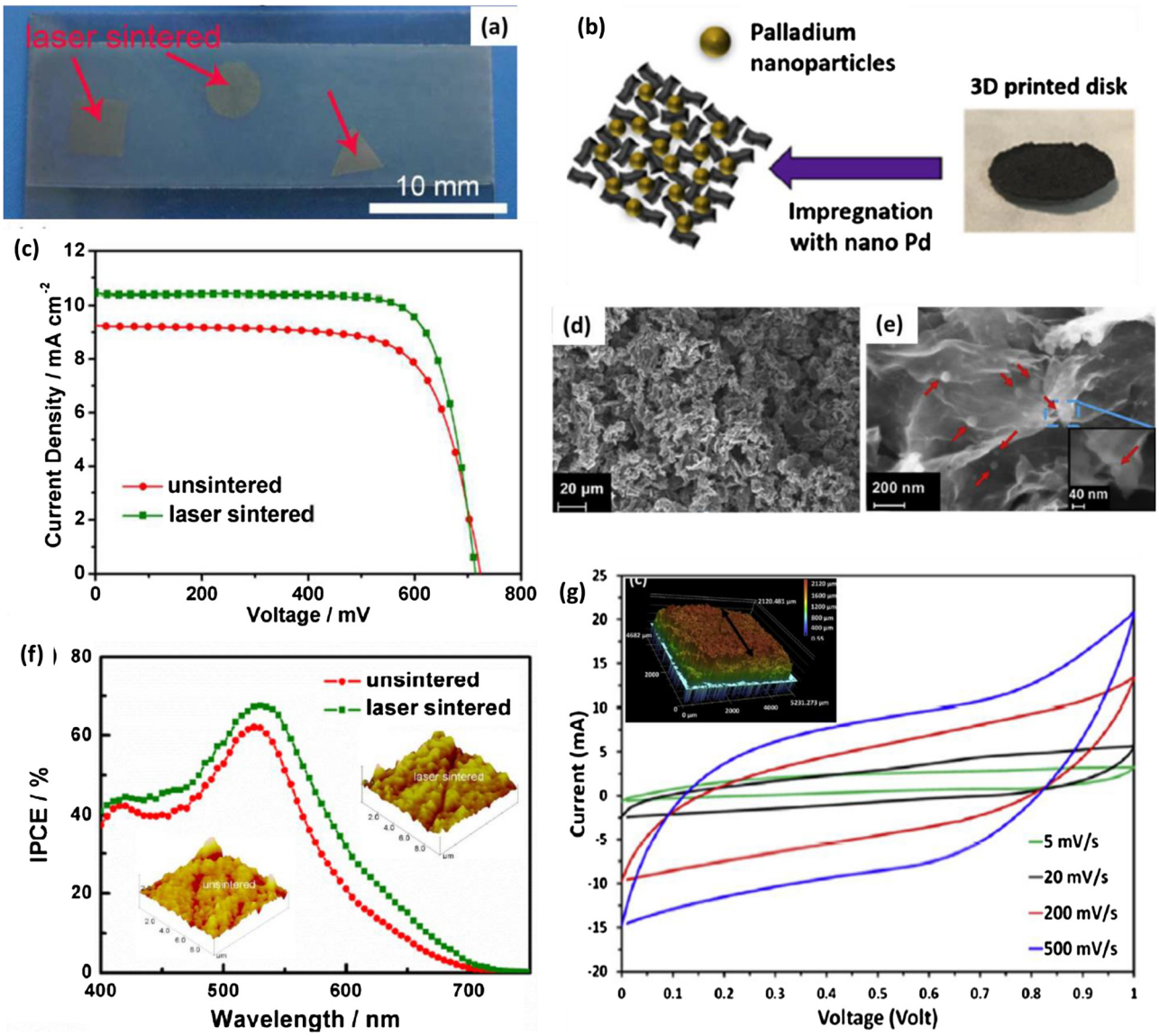

Fig. 15. (a) Optical image of the cold isostatic pressed TiO_2 film on ITOPEN substrate including three laser-sintered patterns [133]. (b) Graphene composites embedded with palladium nanoparticles via binder jetting; the comparison of sintered and unsintered TiO_2 films: (c) current density-voltage and (f) plastic photovoltaics (IPCE) spectra; (d) and (e) SEM images of microstructure graphene composites with palladium nanoparticles; (g) cyclic voltammetry curves of graphene composites at the scan rates of 5, 20, 200, and 500 mV s^{-1} [271]. Copyright 2014 Reproduced by permission of The Royal Society of Chemistry. Copyright 2016 Adapted with permission of Elsevier Inc.

4.3.3. Future trends

Polymeric nanocomposite products fabricated from integrated AM and nanotechnology have demonstrated tremendous potential in water treatment and energy applications due to their hierarchical porosity and large surface-to-volume ratio. In fact, low-dimensional nanomaterials such as covalent/metal organic frameworks, CNTs, graphene and metal oxides have shown great promise as fundamental building blocks for batteries, solar cells, supercapacitors, gas and water ultrafiltration components, etc. [272–276]. New types of non-reactive polymers such as polyvinylidene difluoride (PVDF), polysulfone (PSF), poly (2,6-dimethylphenylene oxide), and poly (phthalazinone ether ketone) are suitable polymeric platforms and matrix materials, applicable in chemically active environments.

By incorporating nanomaterials with polymers or ceramics in either the powder preparation or post-processing stage, AM techniques can provide an effective strategy to engineer 3D porous architectures from the macro- to microscale. The advantages of the resulting functional devices include high energy density, capacity, cycle life and desirable mechanical performance which can withstand large mechanical deformations and avoid fracture or crack propagation. It is also highly possible to achieve printed 3D hierarchical membranes with desirable porous resolution for ultrafiltration and nanofiltration. AM allows for the integration of spiral wound, tubular, plate-and-frame and hollow fibers, which is not possible using conventional techniques.

4.4. Sports equipment and acoustic devices

AM presents itself as a useful means of producing individually customized sports equipment and acoustic devices [277,278]. The use of lightweight, tough and flexible composites with structural topological design has inherent advantages in sports equipment and acoustic devices to engineer stress and sound wave propagation and damping, respectively.

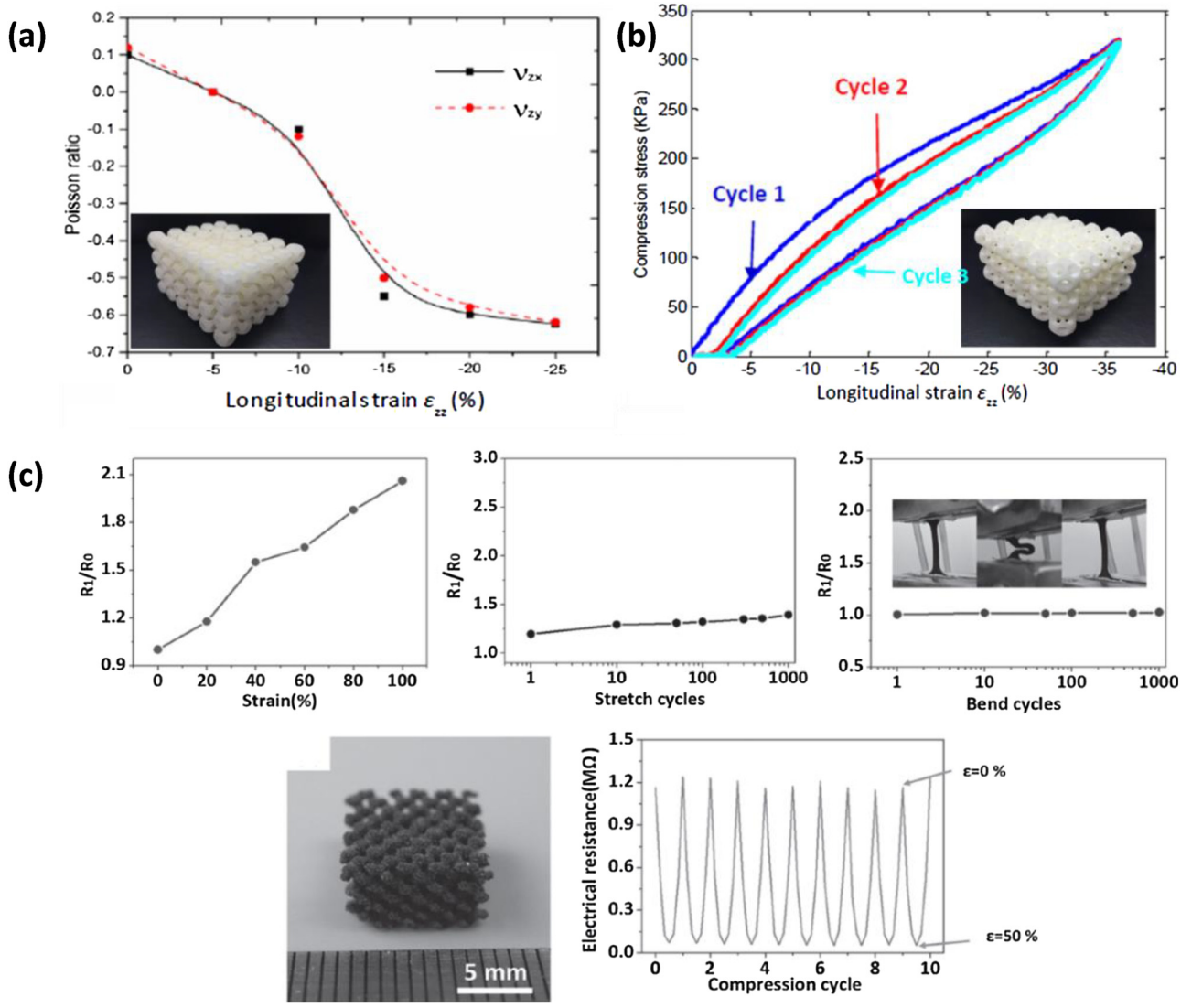

Fig. 16. Auxetic lattice structure upon compressive loading: (a) evolution of the negative Poisson's ratio and (b) cyclic stress-stress curves [51]. (c) Dynamic electromechanical diagrams of CNTs/PU composites [280]. Copyright 2016 Adapted with permission from Elsevier Inc. Copyright 2016 Adapted with permission from John Wiley & Sons, Inc.

4.4.1. Sports equipment

Lightweight and tough frameworks are highly customized and sought after for sports equipment such as sports glasses, golf putters, rackets, bicycles and helmets [279]. Besides the pursued customization design, the mechanical properties such as strength, toughness and ductility of printed parts have also extensively studied at the current stage [70,200]. For instance, Yuan et al. [59] developed CNTs-coated PA12 powders for SLS and achieved laser-sintered composites with excellent specific mechanical strength and toughness. In other works, carbon fibers-reinforced polymers such as micro-carbon fiber/PEEK via SLS exhibited superior mechanical strength over any other composites available in the commercial market [154,195]. Therefore, carbon composites possess unprecedented potential in the application of lightweight and customizable sports equipment.

The usage of soft and flexible materials such as TPE has gained significant attention in shoe and textile manufacturing. Ester-based PU products exhibit high wear resistance, high elasticity and good resistance to oils and solvents. Verbelen et al. and Yuan et al. [46,52,53] evaluated the processability of nanosilica/TPU powders and optimized the process parameters to print complex auxetic lattices via SLS (Fig. 16a). The damping and energy dissipation of printed soft-material products are critical factors influencing their feasibility for use in footwear and protective sports equipment [256,281,282]. Shen et al. [283] applied a hyperelastic model to simulate the strain-stress behaviour of soft PU and predicted the energy absorption capacity of its auxetic lattices upon cyclical compressive loading (Fig. 16b). As shown in Fig. 16c–g, the laser-sintered CNT/PU composite with segregated conductive networks was sensitive to electro-mechanical stimulus [198,260]. This composite material is suitable for damping and sensing applications in wearable devices.

4.4.2. Acoustic devices

Acoustic devices such as sound cloaks, acoustic insulators, waveguides and filters are poised to impact applications ranging from radio frequency communication to medical ultrasound [284,285]. Prior research works mainly rely on microfabrication with complicated procedures (e.g., lithography to prepare 2D patterns or 3D architectures). Experimentally, AM-printed phononic crystals have proven that topological semimetals can provide directional selectivity for filtering incident sound, which enables pseudo-diffusive transport of sound [286]. In Fig. 17, the idea of 3D acoustics via phononic crystals brings topological physics to the macroscopic scale and may lead to potential applications of Weyl phononic crystals in innovative acoustic devices [286].

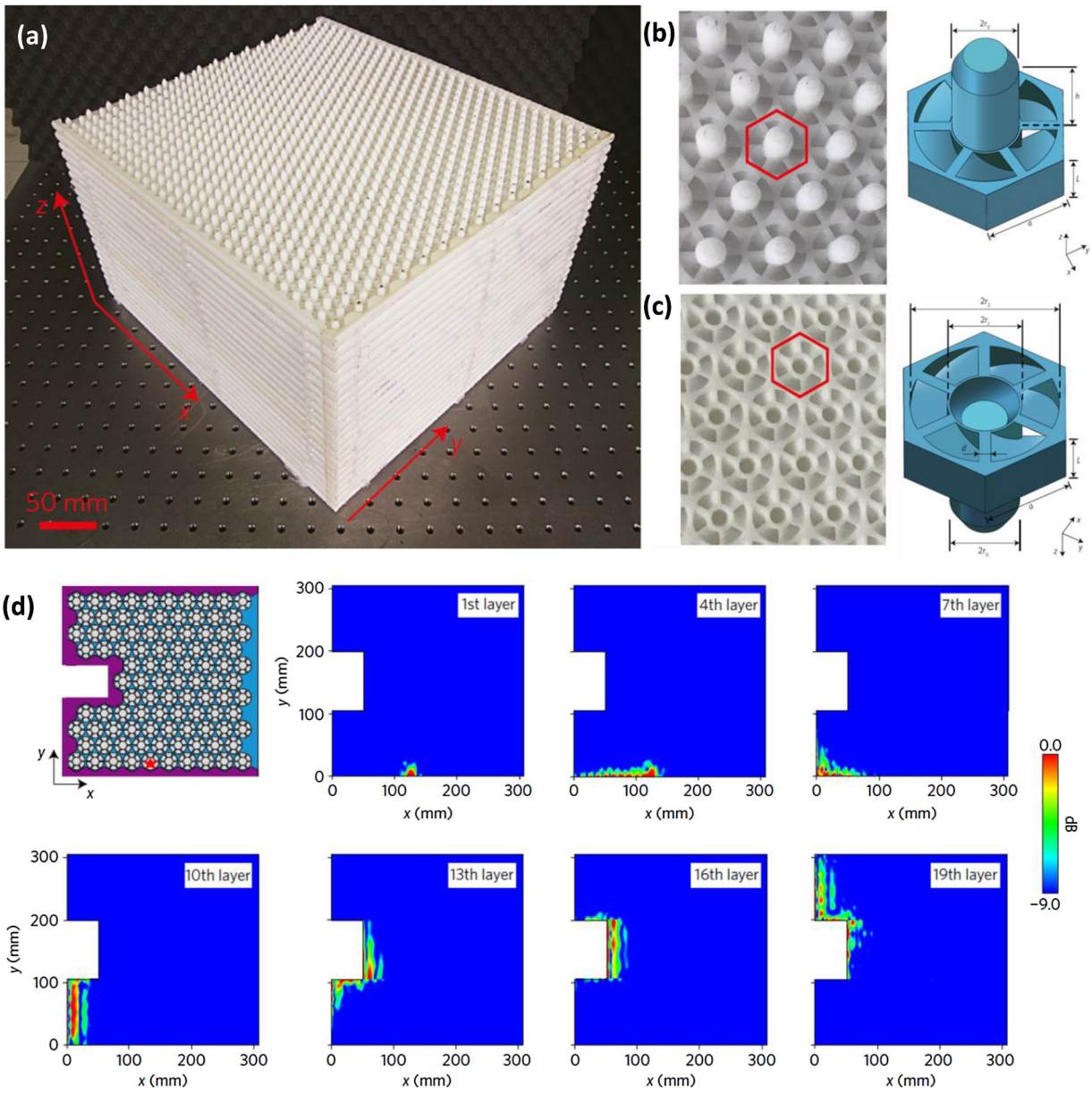

Fig. 17. (a) Illustration of the phononic crystal showing the stacking of the structured plates; (b) and (c) magnified images of the front and back sides of one plate, together with the front and back views of a unit cell; (d) experimental one-way propagation of surface states in the presence of a defect [286]. Copyright 2017 Reproduced with permission from Macmillan publishers limited, part of springer nature.

Sound propagation, scattering and damping in air/solid and solid/solid interfaces follow different principles of controlling elastic waves and acoustic waves. Based on the wave propagation mechanisms, it is desirable to implement 3D acoustic topology in sound insulators and valley acoustics to manipulate soundwave. With the advancement of AM techniques, the morphogenesis of acoustic structures could be effectively realized for functional usages.

4.4.3. Future trends

AM can conveniently achieve effective impact protection and mechanical actuation for sports equipment, compared with other conventional processes such as hot moulding. These applications require structures to undergo large deformation at constant stress and absorb large energy with only a slight increase in strain. The multiple deformation modes (tensile, compression, bending and buckling) and fracture mechanisms of complex AM printed-structures under both dynamic and static loading should be taken into account in a state-of-the-art structural design.

Moreover, complexity of acoustic equipment such as absorbers, filters and guiders rely on multi-phase/multi-element materials with tailored microstructures and architectures. It is vital to pursue a scientific approach that captures the complexity of phonon propagation among materials and the interference by hierarchical structures. This includes modeling of the interactions of constituents in different scaled configurations and 3D acoustic interference induced by structures. For instance, artificial acoustic devices fabricated by AM are able to manipulate sound waves and modulate signals, leading to improved noise attenuation performance [287]. The customized acoustic design can selectively filter sound waves with different frequencies for special applications such as noise shielding and interior voice damping.

In addition, multi-jet fusion is a versatile approach for multi-material printing. Multiple categories of materials such

as conductors, insulators and semiconductors will be achievable through formulating reaction agents with desirable additives and incorporating reinforcement with feeding powders. Progressively, multi-jet fusion will aim to fabricate entirely functional autonomous robots or devices.

5. Conclusion and perspectives

The article provides a review of progress and achievements in the studies of polymeric powder-based AM techniques, ranging from polymers and their composites, powder preparation methods to the properties and applications of printed products. It shows that with their respective unique properties, four categories of reinforcements including metallic, ceramic, carbon-based fillers and organic additives have been widely used to enhance the multi-functionalities of polymeric composites. A variety of single-step and multiple-step powder manufacturing methods have been developed to achieve composite powders with desirable morphologies and compositions. Each method has its specific merits and inevitable disadvantages. The printed multi-functional composite products have exhibited a wide range of interesting mechanical, thermal, electrical, acoustic, bioactive and filtration properties, which have great applications in aerospace, automobile, tissue engineering, drug delivery, water treatment, energy generation, sports equipment and acoustic devices. Moreover, the future trends of different applications are discussed and projected according to the technical challenges and potentials for scientific studies and commercialization.

The traditional approach for AM material research is largely empirical. A rational design approach to develop new polymeric composites with desirable properties and functionalities is usually hampered by a lack of understanding of the effects of composition and process conditions (e.g., thermal and pressure history) on the resulting material structures and macroscopic properties. Numerical modelling has proven to be a useful tool for understanding the forming mechanisms and thermal-mechanical behaviours of materials in AM processes. A multi-physics model that considers the physicochemical properties of polymeric composite powders can reveal and predict the kinetic dynamic behaviours of material fusion, 3D temperature profiles and thermal-induced deformation and residual stresses. Such predictions are able to provide guidance on the design of products (geometry, material and structure) and optimization of AM process parameters including the laser parameters, scanning pattern and building orientation. Meanwhile, the process-structure-property relationships identified for a powder-based AM process can be implemented to control powder morphology and composition so as to engineer the microstructures of printed products and mandate their functional performances.

The challenges for AM-printed materials and structures form the basis for progress in creating knowledge with transformational technological impact. The design of new materials and understanding of their structures and properties are highly expected to afford new capabilities in function and performance. Material optimization involving material formulation and process development is expected to thoroughly facilitate the enhancements of mechanical, electronic, electrochemical, thermal and optical properties of composites. Structural topology will promote basic understanding and ultimately enable advancements within multiple sectors, involving energy, environment, manufacturing, healthcare, mechanics and acoustics.

In the future, an effective integration of AM techniques with other fabrication and treatment methods may provide a multi-process printing to overcome the challenges in precision control, material selection, functional constraints, etc. Multi-process 3D printing including powder-based AM will show numerous advances in the capacity of materials and structures, and strongly extends the functionalities of components or devices.

Acknowledgements

The authors sincerely thank Professor G. C. Berry, Professor K. Matyjaszewski and Professor M. Bockstaller for their invitation and patience in the manuscript preparation. The authors would also like to acknowledge the financial support from the National Research Foundation Medium Sized Center, Singapore through the Marine and Offshore Program. Dr Yuan mainly contributed to the scientific sections; Prof Zhou and Prof Chua supervised the organization of this manuscript; Dr. Shen revised the Figs. 2 and 5.

References

[1] Bose S, Ke D, Sahasrabudhe H, Bandyopadhyay A. Additive manufacturing of biomaterials. Prog Mater Sci 2017;93:45–111.
[2] Chua CK, Leong KF. 3D printing and additive manufacturing: principles and applications. 5th ed World Scientific Publishing; 2017, 456 pp.
[3] Goyanes A, Det-Amornrat U, Wang J, Basit AW, Gaisford S. 3D scanning and 3D printing as innovative technologies for fabricating personalized topical drug delivery systems. J Control Release 2016;234:41–8.
[4] Ligon SC, Liska R, Stampfl J, Gurr M, Mülhaupt R. Polymers for 3D printing and customized additive manufacturing. Chem Rev 2017;117:10212–90.
[5] Parandoush P, Lin D. A review on additive manufacturing of polymer-fiber composites. Compos Struct 2017;182:36–53.
[6] Zheng X, Lee H, Weisgraber TH, Shusteff M, DeOtte J, Duoss EB, et al. Ultralight, ultrastiff mechanical metamaterials. Science 2014;344:1373–7.
[7] Mao Y, Yu K, Isakov MS, Wu J, Dunn ML, Qi HJ. Sequential self-folding structures by 3D printed digital shape memory polymers. Sci Rep 2015;5:13616–28.
[8] Lind JU, Busbee TA, Valentine AD, Pasqualini FS, Yuan H, Yadid M, et al. Instrumented cardiac microphysiological devices via multimaterial three-dimensional printing. Nat Mater 2016;16:303–8.
[9] Chua CK, Leong KF, Tan KH, Wiria FE, Cheah CM. Development of tissue scaffolds using selective laser sintering of polyvinyl alcohol/hydroxyapatite biocomposite for craniofacial and joint defects. J Mater Sci Mater Med 2004;15:1113–21.
[10] Khoo ZX, Teoh JEM, Liu Y, Chua CK, Yang S, An J, et al. 3D printing of smart materials: a review on recent progresses in 4D printing. Virt Phys Prot 2015;10:103–22.
[11] Wehner M, Truby RL, Fitzgerald DJ, Mosadegh B, Whitesides GM, Lewis JA, et al. An integrated design and fabrication strategy for entirely soft, autonomous robots. Nature 2016;536:451–66.
[12] Skylar-Scott MA, Gunasekaran S, Lewis JA. Laser-assisted direct ink writing of planar and 3D metal architectures. Proc Natl Acad Sci USA 2016;113:6137–42.
[13] Goodridge RD, Tuck CJ, Hague RJM. Laser sintering of polyamides and other polymers. Prog Mater Sci 2012;57:229–67.
[14] Zheng X, Smith W, Jackson J, Moran B, Cui H, Chen D, et al. Multiscale metallic metamaterials. Nat Mater 2016;15:1100–6.
[15] Hutmacher DW, Sittinger M, Risbud MV. Scaffold-based tissue engineering: rationale for computer-aided design and solid free-form fabrication systems. Trends Biotechnol 2004;22:354–62.
[16] Taboas JM, Maddox RD, Krebsbach PH, Hollister SJ. Indirect solid free form fabrication of local and global porous, biomimetic and composite 3D polymer-ceramic scaffolds. Biomaterials 2003;24:181–94.
[17] Baumers M, Tuck C, Bourell DL, Sreenivasan R, Hague R. Sustainability of additive manufacturing: measuring the energy consumption of the laser sintering process. J Eng Manuf 2011;225:2228–39.
[18] Manthiram A, Marcus HL, Bourell DL, US 5431967 Selective laser sintering using nanocomposite materials; 1995.
[19] Berry E, Brown JM, Connell M, Craven CM, Efford ND, Radjenovic A, et al. Preliminary experience with medical applications of rapid prototyping by selective laser sintering. Med Eng Phy 1997;19:90–6.
[20] Kruth JP, Wang X, Laoui T, Froyen L. Lasers and materials in selective laser sintering. Assembly Autom 2003;23:357–71.
[21] Sreenivasan R, Bourell DL. Sustainability study in selective laser sintering-an energy perspective. Proc EPD Congress 2010:885–92.
[22] Kim HC, Hahn HT, Yang YS. Synthesis of PA12/functionalized GNP nanocomposite powders for the selective laser sintering process. J Compos Mater 2013;47:501–9.
[23] Pathmanathan K, Johari GP. The effect of increased crystallization on the electrical properties of nylon-12. J Polym Sci Part B Polym Phys 1993;31:265–72.
[24] Schick C. Differential scanning calorimetry (DSC) of semicrystalline polymers. Bioanal Chem 2009;395:1589–611.
[25] Yan C, Shi Y, Yang J, Liu J. A nanosilica/nylon-12 composite powder for selective laser sintering. J Reinf Plast Compos 2009;28:2889–902.

[26] Shi Y, Chen J, Wang Y, Li Z, Huang S. Study of the selective laser sintering of polycarbonate and postprocess for parts reinforcement. J Mater Des Appl 2007;221:37–42.
[27] Shi Y, Wang Y, Chen J, Huang S. Experimental investigation into the selective laser sintering of high-impact polystyrene. J Appl Polym Sci 2008;108:535–40.
[28] Zhang G, Xia Y, Wang H, Tao Y, Tao G, Tu S, et al. A percolation model of thermal conductivity for filled polymer composites. J Compos Mater 2010;44:963–70.
[29] Yuan M, Diller TT, Bourell DL, Beaman J. Thermal conductivity of polyamide 12 powder for use in laser sintering. Rapid Prototyp J 2013;19:437–45.
[30] Han Z, Fina A. Thermal conductivity of carbon nanotubes and their polymer nanocomposites: a review. Prog Polym Sci 2011;36:914–44.
[31] Gaikwad S, Tate JS, Theodoropoulou N, Koo JH. Electrical and mechanical properties of PA11 blended with nanographene platelets using industrial twin-screw extruder for selective laser sintering. J Compos Mater 2012;47:2973–86.
[32] Kawabata A, Murakami T, Nihei M, Yokoyama N. Growth of dense, vertical and horizontal graphene and its thermal properties. Jpn J Appl Phys 2013;52:1–3.
[33] Lao SC, Koo JH, Moon TJ, Londa M, Ibeh CC, Wissler GE, et al. Flame-retardant polyamide 11 nanocomposites: further thermal and flammability studies. J Fire Sci 2011;29:479–98.
[34] Wen S, Yan C, Wei Q, Zhang L, Zhao X, Zhu W, et al. Investigation and development of large-scale equipment and high performance materials for powder bed laser fusion additive manufacturing. Virt Phys Prot 2014;9:213–23.
[35] Farzadi A, Solati-Hashjin M, Asadi-Eydivand M, Osman NAA. Effect of layer thickness and printing orientation on mechanical properties and dimensional accuracy of 3D printed porous samples for bone tissue engineering. PLoS One 2014;9, 108252/1-14.
[36] Castilho M, Moseke C, Ewald A, Gbureck U, Groll J, Pires I, et al. Direct 3D powder printing of biphasic calcium phosphate scaffolds for substitution of complex bone defects. Biofabrication 2014;6, 015006/1-12.
[37] Wu C, Fan W, Zhou Y, Luo Y, Gelinsky M, Chang J, et al. 3D-printing of highly uniform CaSiO3 ceramic scaffolds: preparation, characterization and in vivo osteogenesis. J Mater Chem 2012;22:12288–95.
[38] Calvert P. Inkjet printing for materials and devices. Chem Mater 2001;13:3299–305.
[39] Wood V, Panzer MJ, Chen J, Bradley MS, Halpert JE, Bawendi MG, et al. Inkjet-printed quantum dot–polymer composites for full-color AC-driven displays. Adv Mater 2009;21:2151–5.
[40] Shirazi SFS, Gharenhkhani S, Mehrali M, Yarmand H, Metselaar HSC, Adib Kadri N, et al. A review on powder-based additive manufacturing for tissue engineering: selective laser sintering and inkjet 3D printing. Sci Technol Adv Mater 2015;16:033502–5.
[41] Liu B, Bai P, Li Y. Post treatment process and selective laser sintering mechanism of polymer-coated Mo powder. Open Mater Sci J 2011;5:194–8.
[42] Yan C, Shi Y, Yang J, Liu J. Preparation and selective laser sintering of nylon-12 coated metal powders and post processing. J Mater Process Technol 2009;209:5785–92.
[43] Athreya SR, Kalaitzidou K, Das S. Processing and characterization of a carbon black-filled electrically conductive nylon-12 nanocomposite produced by selective laser sintering. Mater Sci Eng A 2010;527:2637–42.
[44] Chen DZ, Lao SC, Koo JH, Londa M, Alabdullatif Z. Powder processing and properties characterization of polyamide 11-graphene nanocomposites for selective laser sintering. 21st Annu Int Solid Freeform Fabr Symp Proc 2010;vol. 16:435–50.
[45] Shuai C, Feng P, Cao C, Peng S. Processing and characterization of laser sintered hydroxyapatite scaffold for tissue engineering. Biotechnol Bioproc Eng 2013;18:520–7.
[46] Ray SS, Okamoto M. Polymer/layered silicate nanocomposites: a review from preparation to processing. Prog Polym Sci 2003;28:1539–641.
[47] Verbelen L, Dadbakhsh S, Van den Eynde M, Kruth JP, Goderis B, Van Puyvelde P. Characterization of polyamide powders for determination of laser sintering processability. Eur Polym J 2016;75:163–74.
[48] Martin JP. An investigation of the microstructure and properties of a cryogenically mechanically alloyed polycarbonate-poly (ether ether ketone) system. PhD Thesis. Blacksburg: Virgina Polytechnic Institute and State University; 2001, 147 pp.
[49] Plummer K, Vasquez M, Majewski C, Hopkinson N. Study into the recyclability of a thermoplastic polyurethane powder for use in laser sintering. J Eng Manuf 2012;226:1127–35.
[50] Şirin K, Doğan F, Çanlı M, Yavuz M. Mechanical properties of polypropylene (PP) + high-density polyethylene (HDPE) binary blends: non-isothermal degradation kinetics of PP + HDPE (80/20) blends. Polym Adv Technol 2013;24:715–22.
[51] Tan KH, Chua CK, Leong KF, Cheah CM, Gui WS, Tan WS, et al. Selective laser sintering of biocompatible polymers for applications in tissue engineering. Bio Med Mater Eng 2005;15:113–24.
[52] Yuan S, Shen F, Bai J, Chua CK, Wei J, Zhou K. 3D soft auxetic lattice structures fabricated by selective laser sintering: TPU powder evaluation and process optimization. Mater Des 2017;120:317–27.
[53] Dadbakhsh S, Verbelen L, Vandeputte T, Strobbe D, Van Puyvelde P, Kruth JP. Effect of powder size and shape on the SLS processability and mechanical properties of a TPU elastomer. Phys Procedia 2016;83:971–80.
[54] Verbelen L, Dadbakhsh S, Van den Eynde M, Strobbe D, Kruth JP, Goderis B, et al. Analysis of the material properties involved in laser sintering of thermoplastic polyurethane. Addit Manuf 2017;15:12–9.
[55] Schmid M, Wegener K. Thermal and molecular properties of polymer powders for selective laser sintering (SLS). AIP Conf Proc 2016;1779, 100003/1-5.
[56] Shen F, Yuan S, Chua CK, Zhou K. Development of process efficiency maps for selective laser sintering of polymeric composite powders: modeling and experimental testing. J Mater Process Technol 2018;254:52–9.
[57] Laumer T, Stichel T, Raths M, Schmidt M. Analysis of the influence of different flowability on part characteristics regarding the simultaneous laser beam melting of polymers. Phys Procedia 2016;83:937–46.
[58] Schmid M, Amado F, Levy G, Wegener K. Flowability of powders for selective laser sintering (SLS) investigated by round robin test. In: Proc 6th Int Conf Adv Res Virtual and Rapid Prototyp; 2013. p. 95–9.
[59] Schmidt J, Sachs M, Blümel C, Winzer B, Toni F, Wirth KE, et al. A novel process route for the production of spherical LBM polymer powders with small size and good flowability. Powder Technol 2014;261:78–86.
[60] Yuan S, Bai J, Chua C, Wei J, Zhou K. Material evaluation and process optimization of CNT-coated polymer powders for selective laser sintering. Polymers 2016;8:370–7.
[61] Vasquez M, Haworth B, Hopkinson N. Methods for quantifying the stable sintering region in laser sintered polyamide-12. Polym Eng Sci 2013;53:1230–40.
[62] Laumer T, Stichel T, Nagulin K, Schmidt M. Optical analysis of polymer powder materials for selective laser sintering. Polym Test 2016;56:207–13.
[63] Yan W, Lin S, Kafka OL, Lian Y, Yu C, Liu Z, et al. Data-driven multi-scale multi-physics models to derive process–structure–property relationships for additive manufacturing. Comput Mech 2018 2018:1–21.
[64] Tian X, Peng G, Yan M, He S, Yao R. Process prediction of selective laser sintering based on heat transfer analysis for polyamide composite powders. Int J Heat Mass Transfer 2018;120:379–86.
[65] Beal VE, Paggi RA, Salmoria GV, Lago A. Statistical evaluation of laser energy density effect on mechanical properties of polyamide parts manufactured by selective laser sintering. J Appl Polym Sci 2009;113:2910–9.
[66] Rimell JT, Marquis PM. Selective laser sintering of ultra high molecular weight polyethylene for clinical applications. J Biomed Mater Res 2000;53:414–20.
[67] Peyre P, Rouchausse Y, Defauchy D, Régnier G. Experimental and numerical analysis of the selective laser sintering (SLS) of PA12 and PEKK semi-crystalline polymers. J Mater Process Technol 2015;225:326–36.
[68] Zhu W, Yan C, Shi Y, Wen S, Liu J, Shi Y. Investigation into mechanical and microstructural properties of polypropylene manufactured by selective laser sintering in comparison with injection molding counterparts. Mater Des 2015;82:37–45.
[69] Gunatillake PA, Adhikari R. Biodegradable synthetic polymers for tissue engineering. Cell Mater 2003;5:16–21.
[70] Mazzoli A. Selective laser sintering in biomedical engineering. Med Biol Eng Comput 2013;51:245–56.
[71] Bai J, Goodridge RD, Hague RJM, Song M. Improving the mechanical properties of laser-sintered polyamide 12 through incorporation of carbon nanotubes. Polym Eng Sci 2013;53:1937–46.
[72] Shi Y, Li Z, Sun H, Huang S, Zeng F. Development of a polymer alloy of polystyrene (PS) and polyamide (PA) for building functional part based on selective laser sintering (SLS). J Mater Des Appl 2004;218:299–306.
[73] Kruth JP, Mercelis P, Van Vaerenbergh J, Froyen L, Rombouts M. Binding mechanisms in selective laser sintering and selective laser melting. Rapid Prototyp J 2005;11:10–21.
[74] Gibson I, Shi D. Material properties and fabrication parameters in selective laser sintering process. Rapid Prototyp J 1997;3:7–9.
[75] Kruth JP, Levy G, Klocke F, Childs THC. Consolidation phenomena in laser and powder-bed based layered manufacturing. CIRP Ann Manuf Tech 2007;56:29–85.
[76] Evans RS, Bourell DL, Beaman JJ, Campbell MI. SLS materials development method for rapid manufacturing. 16th Annu Int Solid Freeform Fabr Symp Proc 2005;vol. 5:184–96.
[77] Murthy NS. Hydrogen bonding, mobility, and structural transitions in aliphatic polyamides. J Polym Sci Part B: Polym Phys 2006;44:1763–82.
[78] Liu Z, Xu S, Xiao B, Xue P, Wang W, Ma Z. Effect of ball-milling time on mechanical properties of carbon nanotubes reinforced aluminum matrix composites. Composites Part A 2012;43:2161–8.
[79] Salmoria GV, Leite JL, Paggi RA. The microstructural characterization of PA6/PA12 blend specimens fabricated by selective laser sintering. Polym Test 2009;28:746–51.
[80] Udipi K, Davé RS, Kruse RL, Stebbins LR. Polyamides from lactams via anionic ring-opening polymerization: 1. Chemistry and some recent findings. Polymer 1997;38:927–38.
[81] Ramesh C. Crystalline transitions in nylon 12. Macromolecules 1999;32:5704–6.
[82] Berretta S, Ghita OR, Evans KE. Morphology of polymeric powders in laser sintering (LS): from polyamide to new PEEK powders. Eur Polym J 2014;59:218–29.
[83] Gan D, Lu S, Wang Z. Synthesis and characterization of poly(ether ketone ketone) (PEKK)/sodium sulfonated poly (arylene ether ketone)(S-PAEK) block copolymers. Polym Int 2001;50:812–6.

[84] Wang J, Liu Z. Ionic liquids as green reaction media for synthesis of poly(aryl ether ketone)s. Chin Sci Bull 2013;58:1262–6.
[85] Berretta S, Evans KE, Ghita OR. Predicting processing parameters in high temperature laser sintering (HT-LS) from powder properties. Mater Des 2016;105:301–14.
[86] Berretta S, Evans KE, Ghita OR. Processability of PEEK, a new polymer for in high temperature laser sintering (HT-LS). Eur Polym J 2015;68:243–66.
[87] Berretta S, Wang Y, Davies R, Ghita OR. Polymer viscosity, particle coalescence and mechanical performance in high-temperature laser sintering. J Mater Sci 2016;51:4778–94.
[88] Ghita OR, James E, Trimble R, Evans KE. Physico-chemical behaviour of poly (ether ketone)(PEK) in high temperature laser sintering (HT-LS). J Mater Process Technol 2014;214:969–78.
[89] Schmidt M, Pohle D, Rechtenwald T. Selective laser sintering of PEEK. CIRP Ann Manuf Tech 2007;56:205–8.
[90] Gan D, Cao W, Song C, Wang Z. Mechanical properties and morphologies of poly(ether ketone ketone)/glass fibers/mica ternary composites. Mater Lett 2001;51:120–4.
[91] Belbin GR, Staniland PA. Advanced thermoplastics and their composites. Philos Trans R Soc Lond A 1987;322:451–64.
[92] Vasconcelos GC, Mazur RL, Botelho EC, Rezende MC, Costa ML. Evaluation of crystallization kinetics of poly (ether-ketone-ketone) and poly (ether-ether-ketone) by DSC. J Aerosp Technol Manag 2010;2:7–9.
[93] Parvaiz MR, Mohanty S, Nayak SK, Mahanwar PA. Effect of surface modification of fly ash on the mechanical, thermal, electrical and morphological properties of polyetheretherketone composites. Mater Sci Eng A 2011;528:4277–86.
[94] Edwards SL, Werkmeister JA. Mechanical evaluation and cell response of woven polyetheretherketone scaffolds. J Biomed Mater Res A 2012;100A:3326–31.
[95] McLauchlin AR, Ghita OR, Savage L. Studies on the reprocessability of poly (ether ether ketone) (PEEK). J Mater Process Technol 2014;214:75–80.
[96] De Rosa C, Auriemma F, Di Girolamo R, Ruiz de Ballesteros O, Pepe M, Tarallo O, et al. Morphology and mechanical properties of the mesomorphic form of isotactic polypropylene in stereodefective polypropylene. Macromolecules 2013;46:5202–14.
[97] Bellón JM, Buján J, Contreras LA, Jurado F. Use of nonporous polytetrafluoroethylene prosthesis in combination with polypropylene prosthetic abdominal wall implants in prevention of peritoneal adhesions. J Biomed Mater Res 1997;38:197–202.
[98] Fiedler L, Garcia Correa LO, Radusch HJ, Wutzler A, Gerken J. Evaluation of polypropylene powder grades in consideration of the laser sintering processability. J Plas Technol 2007;3:14–7.
[99] Wegner A. New polymer materials for the laser sintering process: polypropylene and others. Phys Procedia 2016;83:1003–12.
[100] Ho HCH, Gibson I, Cheung WL. Effects of energy density on morphology and properties of selective laser sintered polycarbonate. J Mater Process Technol 1999;89:204–10.
[101] Nelson JC, Xue S, Barlow JW, Beaman JJ, Marcus HL, Bourell DL. Model of the selective laser sintering of bisphenol—a polycarbonate. Ind Eng Chem Res 1993;32:2305–17.
[102] Chantarapanich N, Puttawibul P, Sucharitpwatskul S, Jeamwatthanachai P, Inglam S, Sitthiseripratip K. Scaffold library for tissue engineering: a geometric evaluation. Comput Math Methods Med 2012;2012:14–6.
[103] Gorna K, Gogolewski S. Preparation, degradation, and calcification of biodegradable polyurethane foams for bone graft substitutes. J Biomed Mater Res A 2003;67A:813–27.
[104] Yeong WY, Sudarmadji N, Yu HY, Chua CK, Leong KF, Venkatraman SS, et al. Porous polycaprolactone scaffold for cardiac tissue engineering fabricated by selective laser sintering. Acta Biomater 2010;6:2028–34.
[105] Hussain F, Hojjati M, Okamoto M, Gorga RE. Review article: polymer-matrix nanocomposites, processing, manufacturing, and application: an overview. J Compos Mater 2006;40:48–88.
[106] Cardon L, Deckers J, Verberckmoes A, Ragaert K, Delva L, Shahzad K, et al. Polystyrene-coated alumina powder via dispersion polymerization for indirect selective laser sintering applications. J Appl Polym Sci 2013;128:2121–8.
[107] Mazzoli A, Moriconi G, Pauri MG. Characterization of an aluminum-filled polyamide powder for applications in selective laser sintering. Mater Des 2007;28:993–1000.
[108] Zhang Z, Breidt C, Chang L, Friedrich K. Wear of PEEK composites related to their mechanical performances. Tribol Int 2004;37:271–7.
[109] Datsyuk V, Trotsenko S, Reich S. Carbon-nanotube–polymer nanofibers with high thermal conductivity. Carbon 2013;52:605–8.
[110] Klammert U, Gbureck U, Vorndran E, Rödiger J, Meyer-Marcotty P, Kübler AC. 3D powder printed calcium phosphate implants for reconstruction of cranial and maxillofacial defects. J Craniomaxillofac Surg 2010;38:565–70.
[111] Bai P, Li M, Fang M, Cheng J. Study on selective laser sintering mechanism of polymer-coated stainless steel powder. J Mater Eng 2005;0:28–31.
[112] Bai P, Wang W. Selective laser sintering mechanism of polymer-coated molybdenum powder. T Nonferr Metal Soc 2007;17:543–7.
[113] Song YA, Koenig W. Experimental study of the basic process mechanism for direct selective laser sintering of low-melting metallic powder. CIRP Ann Manuf Tech 1997;46:127–30.
[114] Shahzad K, Deckers J, Boury S, Neirinck B, Kruth JP, Vleugels J. Preparation and indirect selective laser sintering of alumina/PA microspheres. Ceram Int 2012;38:1241–7.
[115] Kuo MC, Tsai CM, Huang JC, Chen M. PEEK composites reinforced by nano-sized SiO2 and Al2O3 particulates. Mater Chem Phys 2005;90:185–95.
[116] Deckers J, Kruth JP, Cardon L, Shahzad K, Vleugels J. Densification and geometrical assessments of alumina parts produced through indirect selective laser sintering of alumina-polystyrene composite powder. Strojniški vestnik-J Mech Eng 2013;59:646–61.
[117] Tang HH, Chiu ML, Yen HC. Slurry-based selective laser sintering of polymer-coated ceramic powders to fabricate high strength alumina parts. J Eur Ceram Soc 2011;31:1383–8.
[118] Kenzari S, Bonina D, Dubois JM, Fournée V. Quasicrystal–polymer composites for selective laser sintering technology. Mater Des 2012;35:691–5.
[119] Shahzad K, Deckers J, Zhang Z, Kruth JP, Vleugels J. Additive manufacturing of zirconia parts by indirect selective laser sintering. J Eur Ceram Soc 2014;34:87–95.
[120] Wahab MS, Dalgarno KW, Cochrane RF, Hassan S. Development of polymer nanocomposites for rapid prototyping process. Proc World Congr Eng 2007;9:367–476.
[121] Wang J, Bai P, Zhang Z, Li Y. Processing and characterization of core-shell PA12/Silica composites produced by selective laser sintering. Adv Mat Res 2011;160:756–61.
[122] Qi F, Chen N, Wang Q. Preparation of PA11/BaTiO3 nanocomposite powders with improved processability, dielectric and piezoelectric properties for use in selective laser sintering. Mater Des 2017;131:135–43.
[123] Hon KKB, Gill TJ. Selective laser sintering of SiC/polyamide composites. CIRP Ann Manuf Tech 2003;52:173–6.
[124] Nelson JC, Vail NK, Barlow JW, Beaman JJ, Bourell DL, Marcus HL. Selective laser sintering of polymer-coated silicon carbide powders. Ind Eng Chem Res 1995;34:1641–51.
[125] Yang J, Shi Y, Yan C. Selective laser sintering of polyamide 12/potassium titanium whisker composites. J Appl Polym Sci 2010;117:2196–204.
[126] Chung H, Das S. Processing and properties of glass bead particulate-filled functionally graded nylon-11 composites produced by selective laser sintering. Mater Sci Eng A 2006;437:226–34.
[127] Yan C, Shi Y, Yang J, Liu J. An organically modified montmorillonite/nylon-12 composite powder for selective laser sintering. Rapid Prototyp J 2011;17:28–36.
[128] Wang ZM, Chung TC, Gilman JW, Manias E. Melt-processable syndiotactic polystyrene/montmorillonite nanocomposites. J Polym Sci Part B Polym Phys 2003;41:3173–87.
[129] Wang Y, Shi Y, Huang S. Selective laser sintering of polyamide-rectorite composite. J Mater Des Appl 2005;219:11–6.
[130] Parvaiz MR, Mahanwar PA, Mohanty S, Nayak SK. Effect of surface modification of fly ash reinforced in polyetheretherketone composites. Polym Compos 2011;32:1115–24.
[131] Shishkovsky I, Scherbakov V. Selective laser sintering of biopolymers with micro and nano ceramic additives for medicine. Phys Procedia 2012;39:491–9.
[132] Baumann FE, Monsheimer S, Grebe M, Christoph W, Schiffer T, Scholten H, US 7148286B2 Laser-sintering powder with titanium dioxide particles, process for its preparation, and moldings produced from this laser-sintering powder. Evonik Degussa GmbH; 2006.
[133] Ming L, Yang H, Zhang W, Zeng X, Xiong D, Xu Z, et al. Selective laser sintering of TiO2 nanoparticles film on plastic conductive substrate for highly efficient flexible dye-sensitized solar cell application. J Mater Chem A 2014;2:4566–73.
[134] Zhou WY, Wang M, Cheung WL, Ip WY. Selective laser sintering of poly (L-lactide)/carbonated hydroxyapatite nanocomposite porous scaffolds for bone tissue engineering. In: Eberli D, editor. Tissue engineering. Vienna, Austria: InTech; 2010. p. 179–204.
[135] Zhou WY, Lee SH, Wang M, Cheung WL, Ip WY. Selective laser sintering of porous tissue engineering scaffolds from poly(L-lactide)/carbonated hydroxyapatite nanocomposite microspheres. J Mater Sci Mater Med 2008;19:2535–40.
[136] Duan B, Wang M, Zhou WY, Cheung WL, Li ZY, Lu WW. Three-dimensional nanocomposite scaffolds fabricated via selective laser sintering for bone tissue engineering. Acta Biomater 2010;6:4495–505.
[137] Zhang Y, Hao L, Savalani MM, Harris RA, Di Silvio L, Tanner KE. In vitro biocompatibility of hydroxyapatite-reinforced polymeric composites manufactured by selective laser sintering. J Biomed Mater Res Part A 2009;91:1018–27.
[138] Cruz F. Fabrication of HA/PLLA composite scaffolds for bone tissue engineering using additive manufacturing technologies. In: Elnashar M, editor. Biopolymers. Vienna: InTech; 2011. p. 227–42.
[139] Xia Y, Zhou P, Cheng X, Xie Y, Liang C, Li C, et al. Selective laser sintering fabrication of nano-hydroxyapatite/poly-ε-caprolactone scaffolds for bone tissue engineering applications. Int J Nanomed 2013;8:4197–213.
[140] Wiria FE, Leong KF, Chua CK, Liu Y. Poly-ε-caprolactone/hydroxyapatite for tissue engineering scaffold fabrication via selective laser sintering. Acta Biomater 2007;3:1–12.
[141] Shuai C, Mao Z, Lu H, Nie Y, Hu H, Peng S. Fabrication of porous polyvinyl alcohol scaffold for bone tissue engineering via selective laser sintering. Biofabrication 2013;5, 015014/1-8.

[142] Chu KT, Oshida Y, Hancock EB, Kowolik MJ, Barco T, Zunt SL. Hydroxyapatite/PMMA composites as bone cements. Biomed Mater Eng 2004;14:87–105.
[143] Tanner KE. Bioactive ceramic-reinforced composites for bone augmentation. J R Soc Interface 2010;7:S541–57.
[144] Hao L, Savalani MM, Zhang Y, Tanner KE, Harris RA. Selective laser sintering of hydroxyapatite reinforced polyethylene composites for bioactive implants and tissue scaffold development. J Eng Med 2006;220:521–31.
[145] Liu D, Zhuang J, Shuai C, Peng S. Mechanical properties' improvement of a tricalcium phosphate scaffold with poly-l-lactic acid in selective laser sintering. Biofabrication 2013;5, 025005/1-10.
[146] Chung H, Jee H, Das S. Selective laser sintering of PCL/TCP composites for tissue engineering scaffolds. J Mech Sci Tech 2010;24:241–4.
[147] Lohfeld S, Cahill S, Barron V, McHugh P, Dürselen L, Kreja L, et al. Fabrication, mechanical and in vivo performance of polycaprolactone/tricalcium phosphate composite scaffolds. Acta Biomater 2012;8:3446–56.
[148] Doyle H, Lohfeld S, McHugh P. Predicting the elastic properties of selective laser sintered PCL/β-TCP bone scaffold materials using computational modelling. Ann Biomed Eng 2014;42:661–77.
[149] Simpson RL, Wiria FE, Amis AA, Chua CK, Leong KF, Hansen UN, et al. Development of a 95/5 poly(L-lactide-co-glycolide)/hydroxylapatite and β-tricalcium phosphate scaffold as bone replacement material via selective laser sintering. J Biomed Mater Res B 2008;84:17–25.
[150] Bai J, Goodridge RD, Hague RJM, Song M, Okamoto M. Influence of carbon nanotubes on the rheology and dynamic mechanical properties of polyamide-12 for laser sintering. Polym Test 2014;36:95–100.
[151] Paggi RA, Beal VE, Salmoria GV. Process optimization for PA12/MWCNT nanocomposite manufacturing by selective laser sintering. Int J Adv Manuf Technol 2013;66:1977–85.
[152] Yan C, Hao L, Xu L, Shi Y. Preparation, characterisation and processing of carbon fibre/polyamide-12 composites for selective laser sintering. Compos Sci Technol 2011;71:1834–41.
[153] Zhu W, Yan C, Shi Y, Wen S, Liu J, Wei Q, et al. A novel method based on selective laser sintering for preparing high-performance carbon fibres/polyamide12/epoxy ternary composites. Sci Rep 2016;6:33780–5.
[154] Lao SC, Koo JH, Morgan A, Jor HK, Nguyen K, Wissler G, et al. Flame retardant intumescent polyamide 11-carbon nanofiber nanocomposites: thermal and flammability properties. MRS Symp Proc 2007;1056:3–63.
[155] Chen B, Wang Y, Berretta S, Ghita OR. Poly aryl ether ketones (PAEKs) and carbon-reinforced PAEK powders for laser sintering. J Mater Sci 2017;52:6004–19.
[156] Ho HCH, Cheung WL, Gibson I. Effects of graphite powder on the laser sintering behaviour of polycarbonate. Rapid Prototyp J 2002;8:233–42.
[157] Wang Y, Rouholamin D, Davies R, Ghita OR. Powder characteristics, microstructure and properties of graphite platelet reinforced poly ether ether ketone composites in high temperature laser sintering (HT-LS). Mater Des 2015;88:1310–20.
[158] Salmoria GV, Leite JL, Ahrens CH, Lago A, Pires ATN. Rapid manufacturing of PA/HDPE blend specimens by selective laser sintering: microstructural characterization. Polym Test 2007;26:361–8.
[159] Salmoria GV, Leite JL, Paggi RA, Lago A, Pires ATN. Selective laser sintering of PA12/HDPE blends: effect of components on elastic/plastic behavior. Polym Test 2008;27:654–9.
[160] Schultz JP, Martin JP, Kander RG, Suchicital CTA. Selective laser sintering of nylon 12-PEEK blends formed by cryogenic mechanical alloying. Annu Int Solid Freeform Fabr Symp Proc 2000;5:119–24.
[161] Schultz JP, Martin JP, Kander RG, Suchicital CTA. Processing-structure-property relations of polymer-polymer composites formed by cryogenic mechanical alloying for selective laser sintering applications. MRS Proc 2011;75:1–5.
[162] Bijwe J, Sen S, Ghosh A. Influence of PTFE content in PEEK–PTFE blends on mechanical properties and tribo-performance in various wear modes. Wear 2005;258:1536–42.
[163] Niino T, Yamada H, Seki S. Preliminary study for transparentization of SLS parts by resin infiltration. 5th Annu Int Solid Freeform Fabr Symp Proc 2004;vol. 7:236–43.
[164] Niino T, Yamada H. Transparentization of SLS processed SMMA copolymer parts by infiltrating a thermosetting epoxy resin with tuned refractive index. 16th Annu Int Solid Freeform Fabr Symp Proc 2005;vol. 8:208–16.
[165] Jande YAC. Manufacturing and characterization of uniformly porous and graded porous polymeric structures via selective laser sintering. MS Thesis. Middle East Technical University; 2009. p. 276.
[166] Yan C, Shi Y, Yang J, Liu J. Investigation into the selective laser sintering of styrene–acrylonitrile copolymer and postprocessing. Int J Adv Manuf Technol 2010;51:973–82.
[167] Yang J, Shi Y, Shen Q, Yan C. Selective laser sintering of HIPS and investment casting technology. J Mater Process Technol 2009;209:1901–8.
[168] Ku CWJ, Gibson I, Cheung WL. Selective laser sintered castformtm polystyrene with controlled porosity and its infiltration characteristics by red wax. Annu Int Solid Freeform Fabr Symp Proc 2002;7:107–14.
[169] Booth RB, Thornton BC, Vanelli DL, Gardiner ML, US 8043384B2 Methods and systems for fabricating fire retardant materials. Green Comfort Safe Inc, University of Maine System; 2011.
[170] Salmoria GV, Klauss P, Zepon KM, Kanis LA. The effects of laser energy density and particle size in the selective laser sintering of polycaprolactone/progesterone specimens: morphology and drug release. Int J Adv Manuf Technol 2013;66:1113–8.
[171] Lebovitz AH, Khait K, Torkelson JM. Sub-micron dispersed-phase particle size in polymer blends: overcoming the Taylor limit via solid-state shear pulverization. Polymer 2003;44:199–206.
[172] Tao Y, Kim J, Torkelson JM. Achievement of quasi-nanostructured polymer blends by solid-state shear pulverization and compatibilization by gradient copolymer addition. Polymer 2006;47:6773–81.
[173] Wakabayashi K, Pierre C, Dikin DA, Ruoff RS, Ramanathan T, Brinson LC, et al. Polymer-graphite nanocomposites: effective dispersion and major property enhancement via solid-state shear pulverization. Macromolecules 2008;41:1905–8.
[174] Wakabayashi K, Brunner PJ, Masuda Ji, Hewlett SA, Torkelson JM. Polypropylene-graphite nanocomposites made by solid-state shear pulverization: effects of significantly exfoliated, unmodified graphite content on physical, mechanical and electrical properties. Polymer 2010;51:5525–31.
[175] Kruempel P, Prang H, Kuehl R, Damm E, Eur 3186052A1 Process for preparing a polyolefin composition. Basell Polyolefine GmbH; 2018.
[176] Rydin RW, Maurice D, Courtney TH. Milling dynamics: part I. Attritor dynamics: results of a cinematographic study. Metall Trans A 1993;24:175–85.
[177] Schmidt J, Sachs M, Fanselow S, Zhao M, Romeis S, Drummer D, et al. Optimized polybutylene terephthalate powders for selective laser beam melting. Chem Eng Sci 2016;156:1–10.
[178] Schmidt J, Sachs M, Blümel C, Winzer B, Toni F, Wirth KE, et al. A novel process chain for the production of spherical SLS polymer powders with good flowability. Procedia Eng 2015;102:550–6.
[179] Czekai DA, Seaman LP, Smith DE, US 5662279A Process for milling and media separation; 1997.
[180] Liang SB, Hu DP, Zhu C, Yu AB. Production of fine polymer powder under cryogenic conditions. Chem Eng Technol 2002;25:401–5.
[181] Fan JP, Tsui CP, Tang CY. Modeling of the mechanical behavior of HA/PEEK biocomposite under quasi-static tensile load. Mater Sci Eng A 2004;382:341–50.
[182] Meyer KR, Hornung KH, Feldmann R, Smigerski HJ, US 4334056A Method for polytropically precipitating polyamide powder coating compositions where the polyamides have at least 10 aliphatically bound carbon atoms per carbonamide group. Huels AG; 1982.
[183] Vehring R. Pharmaceutical particle engineering via spray drying. Pharm Res 2008;25:999–1022.
[184] Yeo SD, Kiran E. Formation of polymer particles with supercritical fluids: a review. J Supercrit Fluids 2005;34:287–308.
[185] Mys N, Van De Sande R, Verberckmoes A, Cardon L. Processing of polysulfone to free flowing powder by mechanical milling and spray drying techniques for use in selective laser sintering. Polymers 2016;150:1–16.
[186] Mys N, Verberckmoes A, Cardon L. Processing of syndiotactic polystyrene to microspheres for part manufacturing through selective laser sintering. Polymers 2016;8:383–92.
[187] Bai J, Goodridge RD, Yuan S, Zhou K, Chua C, Wei J. Thermal influence of CNT on the polyamide 12 nanocomposite for selective laser sintering. Molecules 2015;20:19041–61.
[188] Fanselow S, Emamjomeh SE, Wirth KE, Schmidt J, Peukert W. Production of spherical wax and polyolefin microparticles by melt emulsification for additive manufacturing. Chem Eng Sci 2016;141:282–92.
[189] Brunner PJ, Clark JT, Torkelson JM, Wakabayashi K. Processing-structure-property relationships in solid-state shear pulverization: parametric study of specific energy. Polym Eng Sci 2012;52:1555–64.
[190] Eshraghi S, Karevan M, Kalaitzidou K, Das S. Processing and properties of electrically conductive nanocomposites based on polyamide-12 filled with exfoliated graphite nanoplatelets prepared by selective laser sintering. Int J Precis Eng Manuf 2013;14:1947–51.
[191] Chung H, Das S. Functionally graded nylon-11/silica nanocomposites produced by selective laser sintering. Mater Sci Eng A 2008;487:251–7.
[192] Lee G. Selective laser sintering of calcium phosphate materials for orthopedic implants. Ph.D Thesis. Austin: The University of Texas at Austin; 1997. p. 266.
[193] Reisenauer C, Kirschniak A, Drews U, Wallwiener D. Anatomical conditions for pelvic floor reconstruction with polypropylene implant and its application for the treatment of vaginal prolapse. Eur J Obstet Gynecol Reprod Biol 2007;131:214–25.
[194] Fischer S, Pfister A, Galitz V, Lyons B, Robinson C, Rupel K, et al. A high-performance material for aerospace applications: development of carbon fiber filled PEKK for laser sintering. 26th Annu Int Solid Freeform Fabr Symp Proc 2016;vol. 5:34–8.
[195] Yan M, Tian X, Peng G, Li D, Zhang X. High temperature rheological behavior and sintering kinetics of CF/PEEK composites during selective laser sintering. Compos Sci Technol 2018;165:140–7.
[196] Denault J, Dumouchel M. Consolidation process of PEEK/carbon composite for aerospace applications. Adv Perform Mater 1998;5:83–96.
[197] Li CS, Vannabouathong C, Sprague S, Bhandari M. The use of carbon-fiber-reinforced (CFR) PEEK material in orthopedic implants: a systematic review. Clin Med Insights Arthritis Musculoskelet Disord 2015;8:33–45.

[198] Aage N, Andreassen E, Lazarov BS, Sigmund O. Giga-voxel computational morphogenesis for structural design. Nature 2017;550:84–6.
[199] Yuan S, Zhen Y, Chua CK, Yan Q, Zhou K. Electrical and thermal conductivities of MWCNT/polymer composites fabricated by selective laser sintering. Composites Part A 2018;105:203–13.
[200] Bai J, Yuan S, Shen F, Zhang B, Chua CK, Zhou K, et al. Toughening of polyamide 11 with carbon nanotubes for additive manufacturing. Virt Phys Prot 2017;12:235–40.
[201] Pang H, Xu L, Yan DX, Li ZM. Conductive polymer composites with segregated structures. Prog Polym Sci 2014;39:1908–33.
[202] Mohammed HAS. Electrical and electromagnetic interference shielding characteristics of GNP/UHMWPE composites. J Phys D 2016;49, 195302/1-7.
[203] Wu Y, Wang Z, Liu X, Shen X, Zheng Q, Xue Q, et al. Ultralight graphene foam/conductive polymer composites for exceptional electromagnetic interference shielding. ACS Appl Mater Interfaces 2017;9:9059–69.
[204] Morgan AB, Wilkie CA. Flame retardant polymer nanocomposites. Hoboken: John Wiley & Sons Inc; 2007. p. 421.
[205] Huang N, Chen Z, Wang J, Wei P. Synergistic effects of sepiolite on intumescent flame retardant polypropylene. Express Polym Lett 2010;4:9–13.
[206] Levchik SV, Weil ED. A review of recent progress in phosphorus-based flame retardants. J Fire Sci 2006;24:345–64.
[207] Weil ED. Phosphorus-based flame retardants. In: Lewin M, Atlas SM, Pearce IM, editors. Flame-retardant polymeric materials, Vol 2. Boston: Springer; 1978. p. 103–31.
[208] Lao SC, Koo JH, Yong W, Lam C, Zhou J, Moon T, et al. Polyamide 11-carbon nanotubes nanocomposites: preliminary investigation. 19th Annu Int Solid Freeform Fabr Symp Proc 2008;Vol. 1:67–8.
[209] Yi X, Tan ZJ, Yu WJ Li J, Li BJ, Huang BY, et al. Three dimensional printing of carbon/carbon composites by selective laser sintering. Carbon 2016;96:603–7.
[210] Bryning MB, Milkie DE, Islam MF, Kikkawa JM, Yodh AG. Thermal conductivity and interfacial resistance in single-wall carbon nanotube epoxy composites. Appl Phys Lett 2005;87, 161909/1-3.
[211] Chang CM, Liu YL. Electrical conductivity enhancement of polymer/multiwalled carbon nanotube (MWCNT) composites by thermally-induced defunctionalization of MWCNTs. ACS Appl Mater Interfaces 2011;3:2204–8.
[212] Kim GH, Lee D, Shanker A, Shao L, Kwon MS, Gidley D, et al. High thermal conductivity in amorphous polymer blends by engineered interchain interactions. Nat Mater 2015;14:295–300.
[213] Singh V, Bougher TL, Weathers A, Cai Y, Bi K, Pettes MT, et al. High thermal conductivity of chain-oriented amorphous polythiophene. Nat Nanotech 2014;9:384–90.
[214] Xiao Y, Wang W, Lin T, Chen X, Zhang Y, Yang J, et al. Largely enhanced thermal conductivity and high dielectric constant of poly(vinylidene fluoride)/boron nitride composites achieved by adding a few carbon nanotubes. J Phys Chem C 2016;120:6344–55.
[215] Yuan M, Johnson B, Koo JH, Bourell DL. Polyamide 11-MWNT nanocomposites: thermal and electrical conductivity measurements. J Compos Mater 2013;48:1833–41.
[216] Türk DA, Brenni F, Zogg M, Meboldt M. Mechanical characterization of 3D printed polymers for fiber reinforced polymers processing. Mater Des 2017;118:256–65.
[217] Choi JY, Choi JH, Kim NK, Kim Y, Lee JK, Kim MK, et al. Analysis of errors in medical rapid prototyping models. Int J Oral Maxillofac Surg 2002;31:23–32.
[218] Kim SH, Choi YS, Hwang EH, Chung KR, Kook YA, et al. Surgical positioning of orthodontic mini-implants with guides fabricated on models replicated with cone-beam computed tomography. Am J Orthod Dentofacial Orthop 2007;131:S82–9.
[219] Ibrahim D, Broilo TL, Heitz C, De Oliveira MG, De Oliveira HW, Nobre SM, et al. Dimensional error of selective laser sintering, three-dimensional printing and PolyJet™ models in the reproduction of mandibular anatomy. J Craniomaxillofac Surg 2009;37:167–73.
[220] Silva DN, De Oliveira MG, Meurer E, Meurer MI, Da Silva JVL, Santa-Bárbara A. Dimensional error in selective laser sintering and 3D-printing of models for craniomaxillary anatomy reconstruction. J Craniomaxillofac Surg 2008;36:443–9.
[221] Vincent C, Deaudelin I, Robichaud L, Rousseau J, Viscogliosi C, Talbot LR, et al. Rehabilitation needs for older adults with stroke living at home: perceptions of four populations. BMC Geriatr 2007;7:13–20.
[222] Ciocca L, De Crescenzio F, Fantini M, Scotti R. Rehabilitation of the nose using CAD/CAM and rapid prototyping technology after ablative surgery of squamous cell carcinoma: a pilot clinical report. Int J Oral Maxillofac Implants 2010;25:4–27.
[223] Kang SH, Kim MK, Park WS, Lee SH. Accurate computerised mandibular simulation in orthognathic surgery: a new method for integrating the planned postoperative occlusion model. Br J Oral Maxillofac Surg 2010;48:305–7.
[224] Hananouchi T, Saito M, Koyama T, Hagio K, Murase T, Sugano N, et al. Tailor-made surgical guide based on rapid prototyping technique for cup insertion in total hip arthroplasty. Int J Med Robot 2009;5:164–9.
[225] Leiggener C, Messo E, Thor A, Zeilhofer HF, Hirsch JM. A selective laser sintering guide for transferring a virtual plan to real time surgery in composite mandibular reconstruction with free fibula osseous flaps. Int J Oral Maxillofac Surg 2009;38:187–92.
[226] Kim MS, Hansgen AR, Carroll JD. Use of rapid prototyping in the care of patients with structural heart disease. Trends Cardiovasc Med 2008;18:210–6.
[227] Dhandayuthapani B, Yoshida Y, Maekawa T, Kumar DS. Polymeric scaffolds in tissue engineering application: a review. Int J Polym Sci 2011;19:1–18.
[228] Yang S, Leong KF, Du Z, Chua CK. The design of scaffolds for use in tissue engineering. Part I. Traditional factors. Tissue Eng 2001;7:10–6.
[229] Yang S, Leong KF, Du Z, Chua CK. The design of scaffolds for use in tissue engineering. Part II. Rapid prototyping techniques. Tissue Eng 2002;8:11–7.
[230] Khang D, Choi J, Im YM, Kim YJ, Jang JH, Kang SS, et al. Role of subnano-, nano- and submicron-surface features on osteoblast differentiation of bone marrow mesenchymal stem cells. Biomaterials 2012;33:5997–6007.
[231] Champion E. Sintering of calcium phosphate bioceramics. Acta Biomater 2013;9:5855–75.
[232] Sudarmadji N, Tan JY, Leong KF, Chua CK, Loh YT. Investigation of the mechanical properties and porosity relationships in selective laser-sintered polyhedral for functionally graded scaffolds. Acta Biomater 2011;7:530–7.
[233] Cheah CM, Chua CK, Leong KF, Chua SW. Development of a tissue engineering scaffold structure library for rapid prototyping. Part 1: investigation and classification. Int J Adv Manuf Technol 2003;21:291–301.
[234] Naing MW, Chua CK, Leong KF, Wang Y. Fabrication of customised scaffolds using computer-aided design and rapid prototyping techniques. Rapid Prototyp J 2005;11:249–59.
[235] Eshraghi S, Das S. Mechanical and microstructural properties of polycaprolactone scaffolds with one-dimensional, two-dimensional, and three-dimensional orthogonally oriented porous architectures produced by selective laser sintering. Acta Biomater 2010;6:2467–76.
[236] Thieringer FM, Sharma N, Mootien A, Schumacher R, Honigmann P. Patient specific implants from a 3D printer–an innovative manufacturing process for custom PEEK implants in cranio-maxillofacial surgery. In: Meboldt M, Klahn C, editors. Industrializing additive manufacturing - proceedings of additive manufacturing in products and applications – AMPA 2017. Cham: Springer International Publishing; 2018. p. 308–15.
[237] Kim SS, Utsunomiya H, Koski JA, Wu BM, Cima MJ, Sohn J, et al. Survival and function of hepatocytes on a novel three-dimensional synthetic biodegradable polymer scaffold with an intrinsic network of channels. Ann Surg 1998;228:8–13.
[238] Sherwood JK, Riley SL, Palazzolo R, Brown SC, Monkhouse DC, Coates M, et al. A three-dimensional osteochondral composite scaffold for articular cartilage repair. Biomaterials 2002;23:4739–51.
[239] Place ES, George JH, Williams CK, Stevens MM. Synthetic polymer scaffolds for tissue engineering. Chem Soc Rev 2009;38:1139–51.
[240] Hutmacher DW, Schantz T, Zein I, Ng KW, Teoh SH, Tan KC. Mechanical properties and cell cultural response of polycaprolactone scaffolds designed and fabricated via fused deposition modeling. J Biomed Mater Res 2001;55:203–16.
[241] Bártolo PJ, Almeida HA, Rezende RA, Laoui T, Bidanda B. Advanced processes to fabricate scaffolds for tissue engineering. In: Bidanda B, Bártolo PJ, editors. Vlirltual prototyping & bio manufacturing in medical applications. New York: Springer Science+Business Media LLC; 2008. p. 149–70.
[242] Rezwan K, Chen QZ, Blaker JJ, Boccaccini AR. Biodegradable and bioactive porous polymer/inorganic composite scaffolds for bone tissue engineering. Biomaterials 2006;27:3413–31.
[243] Wiltfang J, Merten HA, Schlegel KA, Schultze-Mosgau S, Kloss FR, Rupprecht S, et al. Degradation characteristics of α and β tri-calcium-phosphate (TCP) in minipigs. J Biomed Mater Res 2002;63:115–21.
[244] Kikuchi M, Koyama Y, Yamada T, Imamura Y, Okada T, Shirahama N, et al. Development of guided bone regeneration membrane composed of β-tricalcium phosphate and poly (l-lactide-co-glycolide-co-ε-caprolactone) composites. Biomaterials 2004;25:5979–86.
[245] Vorndran E, Klarner M, Klammert U, Grover LM, Patel S, Barralet JE, et al. 3D powder printing of β-tricalcium phosphate ceramics using different strategies. Adv Eng Mater 2008;10:B67–71.
[246] Sopyan I, Gunawan Shah QH, Mel M. Fabrication and sintering behavior of zinc-doped biphasic calcium phosphate bioceramics. Mater Manuf Process 2016;31:713–8.
[247] Fielding GA, Bandyopadhyay A, Bose S. Effects of silica and zinc oxide doping on mechanical and biological properties of 3D printed tricalcium phosphate tissue engineering scaffolds. Dent Mater 2012;28:113–22.
[248] Moseke C, Gbureck U. Tetracalcium phosphate: synthesis, properties and biomedical applications. Acta Biomater 2010;6:3815–23.
[249] Moulton SE, Wallace GG. 3-dimensional (3D) fabricated polymer based drug delivery systems. J Control Release 2014;193:27–34.
[250] Goyanes A, Martinez PR, Buanz A, Basit AW, Gaisford S. Effect of geometry on drug release from 3D printed tablets. Int J Pharm 2015;494:657–63.
[251] Yuan J, Zhen P, Zhao H, Chen K, Li X, Gao M, et al. The preliminary performance study of the 3D printing of a tricalcium phosphate scaffold for the loading of sustained release anti-tuberculosis drugs. J Mater Sci 2015;50:2015–138.
[252] Palo M, Holländer J, Suominen J, Yliruusi J, Sandler N. 3D printed drug delivery devices: perspectives and technical challenges. Expert Rev Med Dev 2017;14:685–96.
[253] Goole J, Amighi K. 3D printing in pharmaceutics: a new tool for designing customized drug delivery systems. Int J Pharm 2016;499:376–94.
[254] Zhu W, Li J, Leong YJ, Rozen I, Qu X, Dong R, et al. 3D-printed artificial microfish. Adv Mater 2015;27:4411–7.

[255] Lyons B. Additive manufacturing in aerospace: examples and research outlook. Bridge Front. Eng 2012;42(1):13–9.
[256] Bates SRG, Farrow IR, Trask RS. 3D printed polyurethane honeycombs for repeated tailored energy absorption. Mater Des 2016;112:172–83.
[257] Patel SA, Benzo RP, Slivka WA, Sciurba FC. Activity monitoring and energy expenditure in COPD patients: a validation study. Int J Chron Obstruct Pulmon Dis 2007;4:107–12.
[258] Tian X, Jin J, Yuan S, Chua CK, Tor SB, Zhou K. Emerging 3D-printed electrochemical energy storage devices: a critical review. Adv Energy Mater 2017;7, 1700127/1-17.
[259] Deng L, Guo W, Ngo HH, Zhang X, Wang XC, Zhang Q, et al. New functional biocarriers for enhancing the performance of a hybrid moving bed biofilm reactor–membrane bioreactor system. Bioresour Technol 2016;208: 87–93.
[260] Tan WS, Chua CK, Chong TH, Fane AG, Jia A. 3D printing by selective laser sintering of polypropylene feed channel spacers for spiral wound membrane modules for the water industry. Virt Phys Prot 2016;11:151–8.
[261] Tan WS, Suwarno SR, An J, Chua CK, Fane AG, Chong TH. Comparison of solid, liquid and powder forms of 3D printing techniques in membrane spacer fabrication. J Membr Sci 2017;537:283–96.
[262] Capel AJ, Edmondson S, Christie SDR, Goodridge RD, Bibb RJ, Thurstans M. Design and additive manufacture for flow chemistry. Lab Chip 2013;13:4583–90.
[263] Gurreri L, Tamburini A, Cipollina A, Micale G, Ciofalo M. Flow and mass transfer in spacer-filled channels for reverse electrodialysis: a CFD parametrical study. J Membr Sci 2016;497:300–17.
[264] Li F, Meindersma W, De Haan AB, Reith T. Novel spacers for mass transfer enhancement in membrane separations. J Membr Sci 2005;253:1–12.
[265] Dong Y, Fan SQ, Shen Y, Yang JX, Yan P, Chen YP, et al. A novel bio-carrier fabricated using 3D printing technique for wastewater treatment. Sci Rep 2015;5:12400–4.
[266] Yan M, Tian X, Peng G, Cao Y, Li D. Hierarchically porous materials prepared by selective laser sintering. Mater Des 2017;135:62–8.
[267] Low ZX, Chua YT, Ray BM, Mattia D, Metcalfe IS, Patterson DA. Perspective on 3D printing of separation membranes and comparison to related unconventional fabrication techniques. J Membr Sci 2017;523:596–613.
[268] Lalia BS, Kochkodan V, Hashaikeh R, Hilal N. A review on membrane fabrication: structure, properties and performance relationship. Desalination 2013;326:77–95.
[269] Saffarini RB, Summers EK, Arafat HA, Lienhard VJH. Economic evaluation of stand-alone solar powered membrane distillation systems. Desalination 2012;299:55–62.
[270] Franco A, Lanzetta M, Romoli L. Experimental analysis of selective laser sintering of polyamide powders: an energy perspective. J Clean Prod 2010;18:1722–30.
[271] Azhari A, Marzbanrad E, Yilman D, Toyserkani E, Pope MA. Binder-jet powder-bed additive manufacturing (3D printing) of thick graphene-based electrodes. Carbon 2017;119:257–66.
[272] Kenry, Lim CT. Nanofiber technology: current status and emerging developments. Prog Polym Sci 2017;70:1–17.
[273] Le-Clech P, Chen V, Fane TAG. Fouling in membrane bioreactors used in wastewater treatment. J Membr Sci 2006;284:17–53.
[274] Liu G, Jin W, Xu N. Two-dimensional-material membranes: a new family of high-performance separation membranes. Angew Chem Int Ed 2016;55:13384–97.
[275] Sun P, Wang K, Zhu H. Recent developments in graphene-based membranes: structure, mass-transport mechanism and potential applications. Adv Mater 2016;28:2287–310.
[276] Tao K, Tang LH, Wu J, Lye SW, Chang HL, Miao JM. Investigation of multimodal electret-based MEMS energy harvester with impact-induced nonlinearity. J Microelectromech Syst 2018;27:12–39.
[277] Atzeni E, Salmi A. Economics of additive manufacturing for end-usable metal parts. Int J Adv Manuf Technol 2012;62:1147–55.
[278] Tate JS, Gaikwad S, Theodoropoulou N, Trevino E, Koo JH. Carbon/phenolic nanocomposites as advanced thermal protection material in aerospace applications. J Compos 2013;9:1–9.
[279] Biehler J. The future of 3D printed sports equipment; 2017 [accessed June 2018] https://techvibes.com/2017/05/08/the-future-of-3d-printed-sports-equipment/.
[280] Li Z, Wang Z, Gan X, Fu D, Fei G, Xia H. Selective laser sintering 3D printing: a way to construct 3D electrically conductive segregated network in polymer matrix. Macromol Mater Eng 2017;1700211:1–10.
[281] Bianchi M, Scarpa F. Vibration transmissibility and damping behaviour for auxetic and conventional foams under linear and nonlinear regimes. Smart Mater Struct 2013;22:084010–32.
[282] Yuan S, Bai J, Chua CK, Zhou K, Jun W. Characterization of creeping and shape memory effect in laser sintered thermoplastic polyurethane. J Comput Inf Sci Eng 2016;16, 041007/1-5.
[283] Shen F, Yuan S, Guo Y, Zhao B, Bai J, Qwamizadeh M, et al. Energy absorption of thermoplastic polyurethane lattice structures via 3D printing: modeling and prediction. Int J Appl Mech 2016;8, 1640006/1-13.
[284] Stenger N, Wilhelm M, Wegener M. Experiments on elastic cloaking in thin plates. Phys Rev Lett 2012;108, 014301/1-5.
[285] Popa BI, Zigoneanu L, Cummer SA. Experimental acoustic ground cloak in air. Phys Rev Lett 2011;106, 253901/1-4.
[286] Li F, Huang X, Lu J, Ma J, Liu Z. Weyl points and Fermi arcs in a chiral phononic crystal. Nat Phys 2017;14:30–4.
[287] Xie Y, Shen C, Wang W, Li J, Suo D, Popa BI, et al. Acoustic holographic rendering with two-dimensional metamaterial-based passive phased array. Sci Rep 2016;6:35437–43.